Progress in Natural Science: Materials International 27 (2017) 3–20

Contents lists available at ScienceDirect

Progress in Natural Science: Materials International

journal homepage: www.elsevier.com/locate/pnsmi

Review

The use of metal hydrides in fuel cell applications

Mykhaylo V. Lototskyy[a,*], Ivan Tolj[a,b], Lydia Pickering[a], Cordellia Sita[a], Frano Barbir[b], Volodymyr Yartys[c]

[a] HySA Systems Competence Centre, South African Institute for Advanced Materials Chemistry (SAIAMC), University of the Western Cape, Bellville, South Africa
[b] University of Split, Faculty of Electrical Engineering, Mechanical Engineering and Naval Architecture, Department of Thermodynamics and Heat Engines, Split, Croatia
[c] Institute for Energy Technology, Kjeller, Norway

ARTICLE INFO

Keywords:
Fuel cells
Hydrogen storage
Metal hydrides
Thermal integration
System development

ABSTRACT

This paper reviews state-of-the-art developments in hydrogen energy systems which integrate fuel cells with metal hydride-based hydrogen storage. The 187 reference papers included in this review provide an overview of all major publications in the field, as well as recent work by several of the authors of the review. The review contains four parts. The first part gives an overview of the existing types of fuel cells and outlines the potential of using metal hydride stores as a source of hydrogen fuel. The second part of the review considers the suitability and optimisation of different metal hydrides based on their energy efficient thermal integration with fuel cells. The performances of metal hydrides are considered from the viewpoint of the reversible heat driven interaction of the metal hydrides with gaseous H_2. Efficiencies of hydrogen and heat exchange in hydrogen stores to control H_2 charge/discharge flow rates are the focus of the third section of the review and are considered together with metal hydride – fuel cell system integration issues and the corresponding engineering solutions. Finally, the last section of the review describes specific hydrogen-fuelled systems presented in the available reference data.

1. Introduction

Radical changes in energy policy are necessary in order to reduce the consumption of conventional hydrocarbon energy carriers, *viz.* oil, natural gas and coal. Such changes would not only provide benefits for mankind (relating to the climate and environment), but also economic and political advantages for the countries importing these hydrocarbon fuels. The solution to this problem envisages: (i) higher priority of the development and implementation of energy-saving technologies, and (ii) structural changes in the energy sector with the aim to increase the contribution of power generation without the consumption of hydrocarbons which release CO_2 emissions into the atmosphere [1].

A promising option for small- and medium-scale distributed renewable energy systems is electrochemical energy storage, for example rechargeable batteries or hydrogen and fuel cells. These technologies directly convert chemical energy into electricity and are characterised by overall electrical efficiencies of 50–75% [2]. A distinct advantage of electrochemical energy storage systems is that in comparison to conventional combustion heat engines they are not limited by the Carnot efficiency and, therefore, such efficiencies can be achieved at near ambient temperatures. Advanced hybrid energy storage systems which include fuel cells and batteries are particularly promising [3].

Overall, this review summarises the literature data on fuel cell applications which use metal hydrides (MH), mostly, for the storage and supply of gaseous H_2 fuel. For ease of understanding, the review is broken down into several sections to provide the reader with a full insight into developments in the field of fuel cells and metal hydrides. This is achieved by firstly introducing the existing types of commercially available fuel cells and the potential for metal hydride storage for the different systems. Issues surrounding the thermal integration of different types of metal hydrides and their performance in terms of the reversible heat driven interaction with gaseous hydrogen are then discussed. Heat exchange systems and engineering solutions for controlling hydrogen charge/discharge flow rates for integrated metal hydride – fuel cell systems are covered in the subsequent section. Finally, the last section of the review presents reference data on integrated metal hydride-fuel cell systems from the available literature.

1. An overview of fuel cells and the potential of using metal hydrides.

Peer review under responsibility of Chinese Materials Research Society.
* Corresponding author.
E-mail address: mlototskyy@uwc.ac.za (M.V. Lototskyy).

http://dx.doi.org/10.1016/j.pnsc.2017.01.008
Received 1 October 2016; Accepted 30 November 2016
Available online 04 February 2017

Table 1
Types of fuel cells and their main characteristics.

Electrolyte	Fuel	Oxidant	Anode reaction	Cathode reaction	Type of FC	Operating temperature [°C]	Electrical efficiency [%]	Unit power range [kW]	Applications
OH^- conductive alkaline solution	H_2	O_2 Air[a]	$H_2+2(OH)^-\rightarrow 2H_2O + 2e^-$	$\frac{1}{2}O_2+H_2O + 2e^-\rightarrow 2(OH)^-$	AFC	65–220	45–60	1–100	Space Naval
OH^- conductive alkaline solution	$NaBH_4$	O_2 Air[a]	$BH_4^-+8(OH)^-\rightarrow BO_2^-+6H_2O+8e^-$	$2O_2+4H_2O + 8e^-\rightarrow 8(OH)^-$	DBFC	20–85	30–40	10^{-3}–0.5	Portable
OH^- conductive polymer membrane		H_2O_2		$4H_2O_2+8e^-\rightarrow 8(OH)^-$					
Na^+ conductive polymer membrane									
H^+ conductive polymer membrane	H_2	Air	$H_2\rightarrow 2H^++2e^-$	$\frac{1}{2}O_2+2H^++2e^-\rightarrow H_2O$	LT PEMFC	60–80	40–50	0.05–100	Portable Vehicular Stationary
	H_2	Air			HT PEMFC	150–180	45–50	up to 200	Stationary
	CH_3OH	Air	$CH_3OH + H_2O \rightarrow 6H^++6e^-+CO_2$	$\frac{3}{2}O_2+6H^++6e^-\rightarrow 3H_2O$	DMFC	50–130	20–30	up to 5	Portable
H_3PO_4	H_2	Air	$H_2\rightarrow 2H^++2e^-$	$\frac{1}{2}O_2+2H^++2e^-\rightarrow H_2O$	PAFC	150–220	40–45	5–200[b]	Stationary
CO_3^{2-} conductive molten carbonate	H_2	Air	$H_2+CO_3^{2-}\rightarrow H_2O + CO_2+2e^-$	$\frac{1}{2}O_2+CO_2+2e^-\rightarrow CO_3^{2-}$	MCFC	600–700	45–55	100–2000[c]	Stationary
	CO		$CO + CO_3^{2-}\rightarrow 2CO_2+2e^-$						
O^{2-} conductive ceramics	H_2	Air	$H_2+O^{2-}\rightarrow H_2O + 2e^-$	$\frac{1}{2}O_2+2e^-\rightarrow O^{2-}$	SOFC	600–1000	45–60	2.5–250[c]	Stationary
	CO		$CO + O^{2-}\rightarrow CO_2+2e^-$						
	CH_4		$CH_4+4O^{2-}\rightarrow 2H_2O + CO_2+8e^-$	$2O_2+8e^-\rightarrow 4O^{2-}$					

[a] Presence of CO_2 is not allowed.
[b] MW sized plants.
[c] Plants up to 100 MW.

A fuel cell is an electrochemical device which generates electricity directly from a fuel (hydrogen, methane, alcohols, etc.) and oxidant (mostly, O_2) in one step. During operation simultaneous catalytic reactions take place on the opposite sides of an electrolyte, anode and cathode. The reactions depend on the type of electrolyte and fuel used; typical examples are listed in Table 1 which also presents an overview of performance characteristics for the different types of fuel cells [4–13].

There are several types of fuel cells available and typically they are categorised by both their operating temperature and the type of electrolyte used. The selection of an appropriate fuel cell is, subsequently, largely dependent on the end use and different electrocatalysts for fuel oxidation are used depending on the operating temperature.

Alkaline Fuel Cells (AFC) use either noble or non-noble metals as catalysts and aqueous solutions of potassium hydroxide (KOH) as electrolytes at concentrations of between 30 and 50 wt% for low temperature operation (≤120 °C) and up to 85 wt% for high temperature operation (up to 220 °C). The use of AFC's for terrestrial applications is limited, largely due to their susceptibility to carbonisation of the electrolyte. Careful purification of both the fuel and the oxidant from CO_2 is therefore required to mitigate this.

Direct Borohydride Fuel Cells (DBFC) were initially classed as a subcategory of AFC's in which sodium borohydride ($NaBH_4$) dissolved in the alkaline electrolyte was used as a fuel instead of gaseous H_2. The latter developments also use polymer membrane electrolytes with anion (OH^-) or cation (Na^+) conductivity [6,7]. Advantages of DBFC's include high open circuit voltage, high power density, low operating temperature and the use of non-precious metals (e.g., Ni) as electrocatalysts. DBFC's show high potential in portable applications, e.g., for powering electronics or battery recharging when grid power supply is not available [8].

Low Temperature Proton Exchange Membrane Fuel Cells (LT PEMFC) as well as Direct Methanol Fuel Cells (DMFC) and High Temperature Proton Exchange Membrane Fuel Cells (HT PEMFC) use ion exchange membranes with a fluorinated sulfonic acid polymer as an electrolyte.

LT PEMFC's use platinum as an electrocatalyst on the anode and cathode side so the operating temperature is limited by the polymer and varies between 60 and 80 °C. LT PEMFC's have rapid start up times and are, therefore, considered as very promising candidates for fuel cell vehicle (FCV) applications. Water and heat management must be carefully designed in LT PEMFC. DMFC's are a type of LT PEMFC which use methanol or other alcohols without the need for reforming. DMFC's, together with DBFC's, are ideal for portable application, such as laptops, cameras etc. [8].

HT PEMFC's use a composite material based on Polytetrafluoroethylene (PTFE) or Polybenzimidazole (PBI) for the membrane. HT PEMFC's operate at temperatures above 100 °C which subsequently improves the electrochemical kinetics and simplifies water and thermal management.

Phosphoric Acid Fuel Cells (PAFC) use 100% phosphoric acid as the electrolyte which lowers the water vapour pressure, making water management simple. PAFC's are much less sensitive to CO than PEM FC's and AFC's. PAFC's are mostly utilised in stationary applications.

Molten Carbonate Fuel Cells (MCFC) use a combination of alkali carbonates as the electrolyte material. MCFC's do not require noble metals and instead use nickel on the anode side and nickel oxide on the cathode side. In addition, most of the hydrocarbon fuels can be reformed internally in this type of the fuel cell. MCFC's are typically used for stationary and marine applications where size and long start up times are not an issue.

Solid Oxide Fuel Cells (SOFC) use an electrolyte based on non-porous metal oxide, for example ZrO_2 stabilised with Y_2O_3, and have an operating temperature around 1000 °C. With improved thermal conductivity of the solid electrolytes, the operating temperature can be reduced to 600–800 °C. SOFC's are generally used for stationary power applications.

Most of the types of the fuel cells listed in Table 1 either directly or indirectly use hydrogen as a fuel. There is worldwide belief that due to unlimited resources, high energy density, high efficiency, large technological flexibility and the environmentally friendly nature of the energy conversion process, hydrogen holds great promise as an energy carrier [1,14]. Hydrogen fuel cell technologies offer maximum energy storage densities ranging from 0.33 to 0.51 kWh L^{-1} depending on the hydrogen storage method, while the highest value achieved for rechargeable Li-ion batteries does not exceed 0.14 kWh L^{-1}, and for pumped hydroelectric energy storages the energy storage density is as low as 0.27 Wh L^{-1} [15]. In spite of this, there is still room for improvement with respect to fuel cell performance, durability and cost, as well as to increase of the overall efficiency of energy storage systems based on hydrogen and fuel cells.

At the same time compact, safe and efficient hydrogen storage is still a great challenge, which hinders further market penetration of fuel cell energy technologies. Improvements in hydrogen storage gravimetric and volumetric energy densities are still required.

In the past decades various hydrogen storage technologies have been the subject of intensive R & D worldwide [16–24]. Special attention has been paid to the development of material-based hydrogen storage methods which are characterised by high volumetric hydrogen storage densities, minimal requirements to the supporting infrastructure, safety during operation and service and low energy consumption. Materials based hydrogen storage involves a broad spectrum of different materials in which hydrogen can be densified by adsorption (zeolites, carbon materials, metal-organic frameworks), bulk absorption (e.g., clathrates), or chemical interaction (binary and complex hydrides, amides, various organic compounds, etc).

Metal hydrides (MH) formed by the reversible reaction of gaseous H_2 with a parent hydride forming metal, alloy or intermetallic compound are particularly promising for several end-user applications. The use of MH's allows for a very high volumetric hydrogen storage density to be achieved; 100 g_H L^{-1} and higher in respect to the parent material. Modest H_2 equilibrium pressures at ambient temperatures in combination with the endothermic nature of the MH decomposition results in high intrinsic safety of MH-based hydrogen storage systems. Finally, the ability of extremely wide variations of thermodynamic properties in the hydrogen – metal systems by the variation of composition of the parent material allows for exceptional flexibility in MH based hydrogen storage and supply systems. This enables the system performances to be aligned with the operating conditions (temperatures and H_2 pressures) specified by a customer through various material engineering solutions [21–29].

In general, MH's are used as a medium for storing gaseous hydrogen in fuel cell systems. Conversely, in DBFC's, where the fuel is not H_2 but a complex hydride based on $NaBH_4$, MH's are also used as anode (and, sometimes cathode) catalyst materials [6]. Further, in some applications (e.g., AFC's [30]), MH's can combine the functions of both the hydrogen storage medium and anode catalyst.

Advantages of energy storage systems based on PEM electrolysers, fuel cells and hydrogen storage in MH were shown in ref. [31] for off-grid power applications. The footprint of a MH storage sub-system, including the electrolyser and fuel cell, can be significantly smaller than that of the best Li-ion batteries and is competitive on a mass basis.

2. Thermodynamic properties of metal hydrides and their thermal integration with fuel cells

The reversible interaction of an intermetallic alloy A_yB_z with hydrogen gas can be expressed as:

$$A_yB_z + xH_2 \rightleftarrows A_yB_zH_{2x} + \Delta Q, \quad (1)$$

where, A is usually a group IV or rare-earth metal forming a stable hydride, B is a transition metal which does not form a stable hydride but allows for a decrease in heat, ΔQ, released upon absorption of hydrogen (Reaction 1) [32].

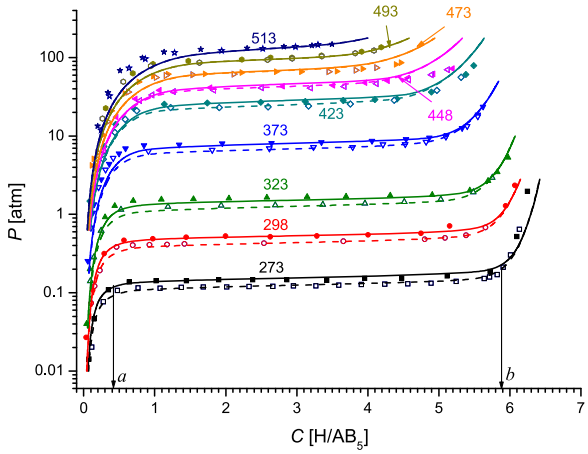

Fig. 1. Experimental points [33] and calculated pressure – composition isotherms [34] for H_2 absorption (filled symbols, solid lines) and desorption (open symbols, dashed lines) in $LaNi_{4.8}Sn_{0.2}$. The temperatures in K are shown in the labels.

From a practical perspective, one of the main considerations for appropriate MH selection is hydrogen pressure (P), which corresponds to the equilibrium of Reaction 1 and is dependent on temperature (T) and hydrogen concentration in the solid (C). As it can be seen from the example presented in Fig. 1, the concentration dependence of the hydrogen equilibrium pressure at a constant temperature (pressure – composition isotherm; PCI) usually has three segments of which the second one exhibits approximately constant H_2 pressure (plateau pressure) and corresponds to the transition of the saturated solid solution of hydrogen in the parent intermetallide (C=a) to an intermetallic hydride (C=b).

The interrelation between pressure, hydrogen concentration and temperature (PCT diagram; Fig. 1) is a characteristic property of a MH material. Precise determination of this dependence has to take into account a number of features, including the temperature-dependent values of a and b, plateau slope and absorption/desorption hysteresis; corresponding modelling approaches have been recently reviewed in ref. [34]. However, in most cases a simplified thermodynamic characterisation of the MH can be used. Here the plateau width, (b–a), is considered as the reversible hydrogen capacity of the material, and the equilibrium of Reaction 1 in the plateau region is described by the van't Hoff equation:

$$\ln P_P = -\frac{\Delta S^o}{R} + \frac{\Delta H^o}{RT}, \quad (2)$$

where, P_P [atm] is the plateau pressure at temperature, T [K]; ΔH^o [J (mol H_2)$^{-1}$] and ΔS^o [J (mol H_2 K)$^{-1}$] are standard enthalpy and entropy changes of the hydriding/dehydriding reaction; and R is the universal gas constant (8.3145 J (mol K)$^{-1}$).

The experimental procedures related to the determination of the thermodynamic properties of MH (PCI, PCT) can be found in a number of publications, including a recent article [35] which describes the thermodynamic characterisation of MH materials loaded in hydrogen storage tanks. This approach can often yield deviations from results collected using smaller laboratory samples [36] due to the presence of steady state temperature gradients in the MH bed [37] within containers. From a practical perspective, the characterisation of PCT properties of MH's in containers is preferable because in general the PCT data is taken at measurement conditions which are comparable to the operating conditions of the end-use application.

The ΔH^o value determines the amount of heat released during the course of hydride formation or absorbed during hydride decomposition (Reaction 1; $\Delta H^o \approx -\Delta Q/x$). It also relates to the changes of plateau pressures with temperature, according to Eq. (2). For example, to reach P=5 bar at T=25 °C, ΔH^o would need to be −28.8 kJ (mol H_2)$^{-1}$, assuming a ΔS^o value of −100 J (mol H_2 K)$^{-1}$ [38].

A simplified schematic representation of the operation of a fuel cell (FC) power module coupled with a MH hydrogen storage and supply system is shown in Fig. 2. In such a system, hydrogen is supplied from the MH system at a pressure, P_{Suppl}, which depends on the MH operating temperature, T_{op}, and can be estimated using Eq. (2). In the FC H_2 is converted to electricity. In doing so, the FC efficiency, η, determines the fraction of chemical energy, W_{Total}, released during the electrochemical oxidation of the fuel into electric energy, W_{el}:

$$\eta = \frac{W_{el}}{W_{Total}}. \quad (3)$$

The existing kinds of FC's (as shown in Table 1) are characterised by various operating temperature ranges and overall efficiencies. As such, $W_{el}=\eta \cdot W_{Total}$, and the remaining energy can be expressed as heat losses, Q_{loss}, dissipated in the environment during FC operation and equal to:

$$Q_{loss} = W_{Total} - W_{el} = W_{Total}(1-\eta). \quad (4)$$

For hydrogen fuelled FC's, heat losses estimated from Eq. (4) can be used to provide the correct hydrogen supply by enabling the decomposition of (inter)metallic hydrides, according to the reverse process of Reaction 1. This process is endothermic and subsequently requires a supply of heat approximately equal to the absolute value of the hydrogenation enthalpy, $|\Delta H^o|$. Assuming W_{Total} to be equal to the higher hydrogen heating value, (HHV=284.36 kJ (mol H_2)$^{-1}$ [4]), we can estimate the conditions at which H_2 supply from the MH to the FC can be provided without additional energy input, i.e. by only utilising heat losses during FC operation:

$$|\Delta H^o| \le Q_{loss} = HHV(1-\eta). \quad (5)$$

Another condition requires the plateau pressure at the operating temperature (Eq. (2)) to be higher than the pressure of hydrogen supply, P_{Suppl}, to the FC stack. The latter value is dependent on design features of the FC Balance of Plant (BoP) and can range from a gage pressure of 100 mbar to several bars H_2 [11], i.e. from 1.1 to ~10 bar absolute. The operation temperature, T_{op}, at which this

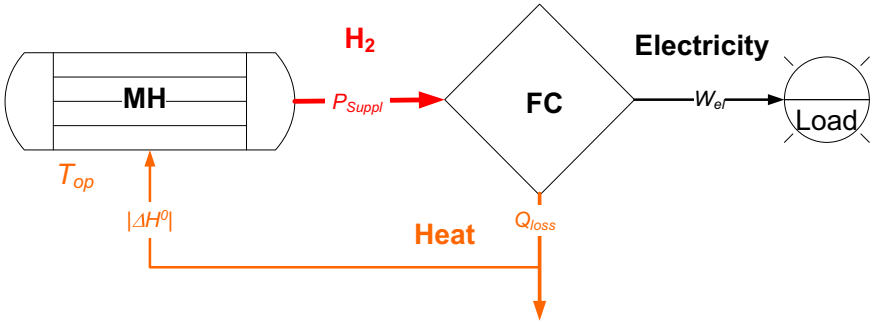

Fig. 2. Schematic representation of the operation of a FC power module coupled with a MH hydrogen storage and supply system.

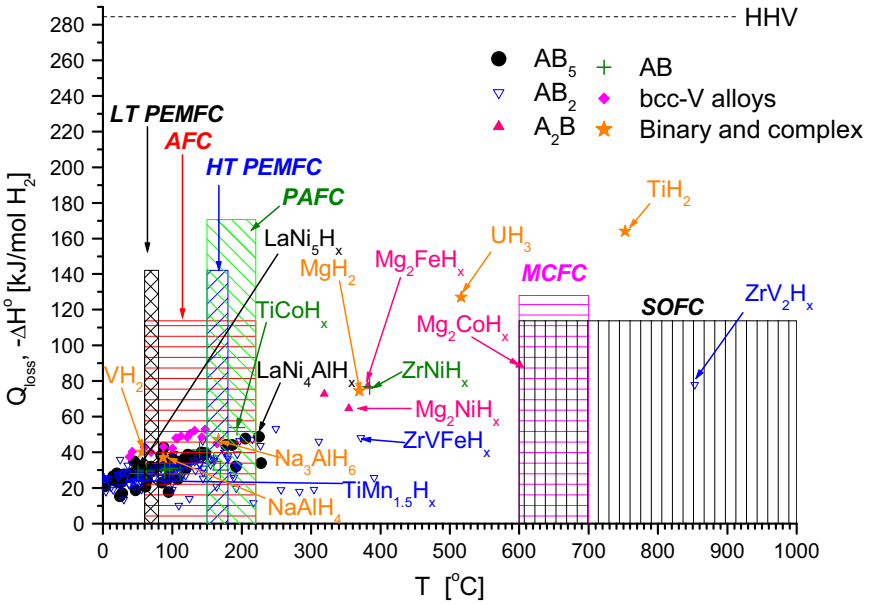

Fig. 3. Potential of various metal hydrides with the associated heat losses (Q_{loss}) in different types of fuel cells. The operation temperatures of the MH's correspond to H_2 plateau pressures of 10 bar.

condition is satisfied can be estimated through the solution of Eq. (2) with respect to T:

$$T_{op} \geq \frac{\Delta H^o}{\Delta S^o + R \ln P_{Suppl}}. \quad (6)$$

The feasibility of thermal integration of a MH material with a hydrogen fuelled FC therefore requires the thermodynamic properties of its reversible interaction with H_2 gas (ΔH^o and ΔS^o) to satisfy Eqs. 5 and 6, where $|\Delta H^o|$ and the operating temperature should fit in the range specific to the particular type of FC. The corresponding estimations, based on reference ΔH^o and ΔS^o values for a number of binary and intermetallic hydrides [29], as well as typical operating parameters of the FC's (Table 1), are presented in Fig. 3, for a plateau pressure of 10 bar. The series showing binary hydrides is supplemented by data on complex hydrides based on $NaAlH_4$ and Na_3AlH_6 which are able to reversibly interact with H_2. Note that because of kinetic limitations these complex hydrides can only operate at $T \geq 150$ °C, which for $NaAlH_4$ corresponds to a plateau pressure above 60 bar H_2 [39] [1].

It can be seen from Fig. 3 that most of the intermetallic hydrides (AB_5, AB_2, and Ti-based AB-types) and pseudo-binary hydrides based on BCC-V alloys, are suitable for low- and moderately high-temperature FC applications, including AFC's, LT- and HT-PEMFC's, and PAFC's. The above-mentioned types of MH's are classed as being suitable for low temperature applications when they demonstrate an equilibrium pressure above atmospheric pressure at temperatures up to 100 °C [21]. Such a class of MH's feature $|\Delta H| < 45$ kJ(mol H_2)$^{-1}$ and high hydrogen sorption/desorption rates. The main drawback to these MH's is their low reversible gravimetric hydrogen capacities – typically not more than 1.5–2 wt%. However, the major advantage of these materials is that small changes in the composition of the alloys significantly influence the pressures at which hydrogen is absorbed and desorbed; low hysteresis and moderate plateau slopes make them suitable for a wide range of applications [29,41,42]. Hydrogen supply from "low-temperature" MH's requires quite modest energy input, from 10–20% of the *HHV*, or 15% to 40–45% of the released heat, Q_{loss}. This means that thermal integration of these materials with the BoP (cooling system) of the FC stack does not require high heat transfer efficiency: it can be achieved using quite simple solutions, e.g. by capturing the warm air from the exhaust of the cooling system of the FC power module [38,43,44].

In cases when the required MH heating temperature should be higher than the FC operating temperature (e.g. when using $NaAlH_4$ for H_2 supply to LT-PEMFC's), special solutions such as catalytic combustion of part of the released H_2 is necessary [40]. This, however, results in a decrease in the system efficiency.

High-temperature FC's (MCFC's, SOFC's) are suitable for operation with both "low-temperature", and some "high-temperature" MH's, including; MgH_2 and Mg-based A_2B hydrogen storage intermetallics, as well as AB_2- and AB-type intermetallides where A=Zr. When utilising the former "low-temperature" group, special attention should be paid to the thermal control of the MH material to avoid its overheating and uncontrolled H_2 pressure increase. For "high-temperature" hydrogen storage materials based on MgH_2 the operating temperature should be limited as well (≤350 °C) to avoid losses in the cycling stability of the material as a result of the Mg sintering at higher temperatures [45]. This undesired effect can be mitigated by the addition of minor amounts of carbon to the material [46]. Another problem is providing fast kinetics for hydrogen absorption/desorption in MgH_2; the most effective way to achieve this is the preparation of nanocomposite materials by ball milling Mg with catalytic additives in hydrogen atmosphere (see [45–47] and references therein).

The use of "high-temperature" MH's allows the system to utilise 60–90% of the released heat, Q_{loss}, which enables the problem of thermal control of the high-temperature FC stack to be overcome. We note that the use of some binary hydrides (e.g., UH_3, TiH_2) for hydrogen supply in such an application would be problematic because these materials have too high hydrogenation heat effects ($|\Delta H^o| > Q_{loss}$) and thus require additional energy input to provide desorption of the required amount of H_2. This would subsequently result in a decrease of the overall system efficiency.

3. Design parameters of efficient metal hydride based systems

The integration of MH's into the BoP of FC systems is firstly related to the selection of an appropriate MH material and, further, its

[1] According to [40], at P=3bar, decomposition of $NaAlH_4$ starts at ~55°C, while decomposition of Na_3AlH_6 starts at ~130°C. However, to provide fast refuelling of hydrogen storage tanks based on sodium alanates, the temperatures and corresponding H_2 pressures should be higher.

Table 2
Examples of FC systems employing MH.

Fuel cell		Metal hydride hydrogen storage			Ref.
		MH Material	Weight		
Type	Power (el.) [kW]		MH [kg]	H_2 stored [kg]	
1	2	3	4	5	6
LT-PEMFC	5	$(Ti,Zr)(V,Cr,Mn,Fe,Al)_2$ / OV679	4×190[(i)]	12	[38]
LT-PEMFC	0.017–1.2	AB_2 (A=Ti+Zr; B=Fe+Mn+Cr+Ni; Ti:Fe=1:1; Ti:Zr=0.55:0.45)	0.07–12.2	0.009–0.17	[43,67]
LT-PEMFC	10	AB_2 (A=Ti+Zr; B=Fe+Mn+Cr+Ni; Ti:Zr=0.65:0.35)	20×3.2	0.9	[44]
LT-PEMFC	1.2	$Ti_{0.98}Zr_{0.02}V_{0.43}Fe_{0.09}Cr_{0.05}Mn_{1.5}$	2×2.2[(i)]	0.044	[53]
LT-PEMFC	14	AB_2 (A=Ti+Zr; B=Mn+Fe+...) (Hydralloy C15 / GfE)	213	2.98	[54]
AFC	[(ii)]	$LmNi_{4.1}Co_{0.4}Mn_{0.4}Al_{0.3}$	[(ii)]		[30]
LT-PEMFC	2	$LaNi_5$	4×4.2	0.252	[55]
LT-PEMFC	0.03	AlH_3[(iii)]	0.4	0.04	[56]
LT-PEMFC	6	$LaNi_5$	4.4	0.046	[57]
LT-PEMFC	0.1	$NaBH_4$ / H_2O[(iii)]	0.5 [(iv)]	0.05	[58]
SOFC	1	MgH_2	1.8	0.107	[59,60]
LT-PEMFC	0.9	MgH_2[(v)]	57[(vi)]	4	[61]
LT-PEMFC	0.05	No data[(vii)]			[62]
LT-PEMFC	16	No data[(viii)]			[63]
LT-PEMFC	0.6	No data[(ix)]		0.134	[64]
LT-PEMFC	80	$LaNi_5$	14×538	130	[65,66]
SOFC	6.7[(x)]	MgH_2	1.75	0.1	[68]
LT-PEMFC	2.3	No data[(xi)]		0.098	[69]
HT-PEMFC	1	2 $LiNH_2$ + 1.1 MgH_2 + 0.1 $LiBH_4$ + 3 wt% $ZrCoH_3$	3	0.135	[70]
LT-PEMFC	240	No data[(ix)]			[71]
LT-PEMFC	2–4	No data [(ix)]		1	[72]
LT-PEMFC	100	No data[(ix)]		200	[73]
LT-PEMFC	1.2	No data[(ix)]; 2x MH cartridges			[74]
LT-PEMFC	10–17	AB_2	No data	2.8–3.5	[75]
LT-PEMFC	10	No data[(ix)]; GfE metal hydride tank		4	[76]
HT-PEMFC	0.26	$NaAlH_4$ + 4 mol% $TiCl_3$	2.7	0.06	[77]
HT-PEMFC	1.2	No data[(ix),(xii)]			[78]
LT-PEMFC	1.5	AB_2 (A=Ti+Zr; B=Fe+Mn+V) AUERSTORE®, Treibacher AG	2×13[(i)]	0.179	[79]
LT-PEMFC	5	No data[(ix)]; Labtech SA metal hydride tank		1.34	[80]
LT-PEMFC	0.05	$MmNi_{4.7}Al_{0.3}$	0.5	0.006	[81]
LT-PEMFC	1	$LaNi_5$	7	0.089	[82]
LT-PEMFC	1	$LaNi_{4.8}Al_{0.2}$	6×4.83	0.279	[83]
LT-PEMFC	0.9–1.1	$LaNi_{4.78}Sn_{0.22}$	2.48	0.025	[84]
LT-PEMFC	5	$MmNi_5$	185	2	[85]
LT-PEMFC	0.03	AB_2	4×0.165[(i)]	0.006	[86]
1	**2**	**3**	**4**	**5**	**6**
HT-PEMFC	30	$NaAlH_4$ (Ti-doped)	22[(vi)]	0.067[(vi)]	[87,88]
LT-PEMFC	0.5–5	La(Ce, Mm)Ni_5	3.6–36[(vi)]	0.054–0.536	[89]
LT-PEMFC	0.6[(x)]	$MmNi_5$	50	0.482[(vi)]	[90,91]
LT-PEMFC	0.2	$Ti_{0.95}Zr_{0.05}Mn_{1.4}Cr_{0.1}V_{0.2}$	6	0.082	[92]
LT-PEMFC	0.2–0.25	$Ml_{0.85}Ca_{0.15}Ni_5$	4.3	0.047[(vi)]	[93]
		$Ti_{0.9}Zr_{0.15}Mn_{1.6}Cr_{0.2}V_{0.2}$	2.9	0.038[(vi)]	
LT-PEMFC	0.5	$Lm_{1.06}Ni_{4.96}Al_{0.04}$ (Lm = La 55%,Ce 2.5%, Pr 7.7%, Nd 34.1%)	27[(vi)]	0.343	[94]
LT-PEMFC	0.2	AB_5	4×4.5 +/−0.2[(i)]	0.045 each, 0.179 total	[95]
LT-PEMFC	0.2–1.1[(vi)]	$Ti_{0.98}Zr_{0.02}V_{0.43}Fe_{0.09}Cr_{0.05}Mn_{1.5}$	No data	0.08	[96]
LT-PEMFC	10	AB_2 (A=Ti+Zr; B=Fe+Cr+Mn+Ni; Ti:Zr=0.65:0.35)	64	0.9	[97]
LT-PEMFC	8.7	$Lm_{1.06}Ni_{4.96}Al_{0.04}$ $Fe_{0.9}Mn_{0.1}Ti$	224[(i)]	2	[98,99]
HT_PEMFC	1	$NaAlH_4$ with Ce catalyst	2	No data	[100]
HT-PEMFC	6	$NaAlH_4$ with Ce catalyst	No data [(xiii)]		[101]
HT-PEMFC	1	$NaAlH_4$ with Ce catalyst	No data		[102]
LT-PEMFC	0.5	$LaNi_5$	6.1×5[(i)]	0.305	[103]
LT-PEMFC	1.2	Ce modified $LaNi_5$	17.5	0.260	[104]
LT-PEMFC	No data	AB_2 (A=Ti+Zr; B=Mn+Fe+...) (Hydralloy C15 / GfE)	No data	0.09	[105]
LT-PEMFC	5	$LaNi_5$	5×0.101	5×0.013 0.065 total	[106]
LT-PEMFC	No data	$Ti_{25}Cr_{50}V_{25}$	4×75	7.3	[107]
SOFC	0.5	MgH_2	No data [(xiii)]		[108]

integration into a MH hydrogen storage tank. The selected MH must enable successful performance of the application, both during H_2 refuelling and FC operation. Furthermore, the MH tank should be coupled with a hydrogen supply and heat management (cooling) systems of the FC power module, as schematically shown in Fig. 2.

Accordingly, this section deals with both MH materials and MH containers as the main components of MH tanks and is followed by a summary of typical layout features for their integration with FC systems.

3.1. Metal hydride materials

As with any system employing hydrogen storage, the requirements of the MH are application specific. For example, a recent review of the properties required by hydrogen storage materials for automotive PEMFC systems includes an intrinsic hydrogen capacity target of > 13.5 wt% at pressures between 5 and 100 bar H_2 at 60–150 °C, an equilibrium pressure > 5 bar H_2 at the minimum system coolant temperature and < 100 bar at ~150 °C [48]. In addition to these targets, along with targets set by various vehicle manufacturers and national bodies (e.g. US DOE [49]), when considering appropriate MH selection for a given application there are several other factors which must be considered, including; uptake/discharge kinetics, hysteresis effects (which affect the system efficiency of certain end-use applications), cyclability, ease of activation, sensitivity to air or other impurities, and cost.

For FC vehicle applications special attention in the material screening criteria for solid state hydrogen storage should also be paid to specific performances, including: (i) volumetric storage capacity, (ii) heat transfer for desorption, (iii) recharging at low temperatures and (iv) cold start of the vehicle [50].

Table 2 provides a summary of MH selection for several different types of FC's, compiled using data from the literature. It is evident from the table that not only are there significantly more examples of MH storage integrated with PEMFC's but also that, in spite of their low gravimetric capacities, intermetallic hydrides based on AB_2 and AB_5 alloys are two of the most utilised MH's for practical applications to date. As previously mentioned (Section 2), the major advantage of this class of MH is that their PCT properties may be tailored/tuned to the pressure and temperature requirements of a given system by making small changes to the alloy composition. For example, previous work on Ti-V based AB_2 MH's has shown that an increase in V content decreases plateau pressure whilst increasing the usable capacity [51] and further, very small changes in V content (~0.05 at%) can lead to significant changes in plateau pressure and hysteresis [52].

SOFC's operate at the highest temperature of all the FC types making them suitable for use with MH storage tanks based on MgH_2 which; has a high hydrogen storage capacity (~7.6 wt%), is widely available, and, is low in cost in comparison to MH's based on AB_2, AB_5 and other intermetallic alloys. A MgH_2 hydrogen storage tank thermally integrated with a 1 kW SOFC stack was developed for a prototype combined heat and power (CHP) unit, utilising electricity generated from renewable energy sources [59]. This development will be discussed further in Section 3.3.

In an attempt to reduce the weight and subsequent cost of MH's, ref [109] investigated the potential for a novel hydrogen storage material based on a transition metal oxide supported on polymeric matrices. In the study, a manganese oxide was linked onto a polymeric matrix based on poly-ether-ether-ketone (PEEK). Following on from their initial study the authors went on to develop a small scale prototype system using the same novel material, which had a known capacity of 1.1 wt% at 100 °C under 60 bar H_2, coupled with a single cell PEMFC [110]. It was found that a 20 g sample of MnO_2 supported on PEEK could provide the PEMFC with 0.2 g of hydrogen, enabling a nominal power output between 6 and 10 W for 400–500 s.

A computational study on the use of Aluminium Hydride, *"Alane"*, as another novel hydrogen storage material for use in a portable LT-PEMFC based power application, was also performed [56]. From a practical viewpoint, the use of Alane within FC systems poses several challenges, of which the most significant is the risk of over-pressurisation of the MH tank during dehydrogenation. As shown in Table 2, it was found that a 30 W PEMFC system could operate for approximately 25 h using 0.4 kg of Alane, which supplied the system with ~0.04 kg of usable hydrogen.

Further, a number of complex hydrides, including Mg_2FeH_6 and $Mg(BH_4)_2$, which are characterised by high weight hydrogen storage densities and potentially low costs were suggested for hydrogen storage in PEM FC systems in ref. [111].

Although ref's [56,109–111] provide a useful insight into the use of novel hydrogen storage media, further work needs to be carried out to demonstrate feasibility of the integration of hydrogen storage tanks based on these materials with the BoP for scaled up systems under 'real' operating conditions.

Given the current limitation of these novel hydrogen storage methods, MH's still provide the best solution for efficient and safe storage of hydrogen for FC applications. For further reading, a review of MH's for solid state hydrogen storage was recently provided by Rusman et al. [112].

3.2. Metal hydride containers

The integration of MH's into FC power systems requires very care consideration to ensure the overall system (FC module + MH hydrogen storage) is able to operate effectively. This involves several different factors. Firstly, the required amount of stored hydrogen fuel to be achieved within the space and weight constrains of a particular application must be ascertained. Secondly, the hydrogen storage system has to provide sufficient H_2 supply to the FC when operating at a maximum rated power for a specified time. Thirdly, H_2 refuelling of the storage system has to take a reasonably short time.

Appropriate selection of the MH material can partially address the first and the second points related to (i) weight and volume hydrogen storage densities and (ii) energy consumption for providing the required H_2 supply from the MH. However, as it was shown in ref. [24], in addition to the MH material-related properties, the specified performances are also affected by the features of the MH containers in which the MH material is placed. Furthermore, the rates of H_2 supply both from MH tank (FC operation) and, especially, to the MH tank (refuelling) will be greatly dependent on the size, geometry and layout of the MH container, particularly, its inner part (MH bed). These dependencies, which are additionally affected by pressure – temperature conditions of the hydrogen absorption/desorption, as well as heat exchange characteristics between the MH and accessories for its heating and cooling, are quite complicated and often require numerical modelling followed by experimental verification.

The design features of MH containers (MH reactors) for various applications were reviewed by Sun in 1992 [113], Yang et. al in 2010 [114] and more recently Shafiee and McCay in 2016 [115]. In addition,

(i) material + containment; (ii) MH was embedded in the fuel cell anode (60–150 $mgcm^{-2}$). The discharge capacity at 50 mAg^{-1} was ~250 $mAhg^{-1}$; (iii) non-rechargeable; (iv) catalytic hydrolysis system utilising 25 wt.% aqueous solution of $NaBH_4$; (v) additional electric heating of the MH tank; (vi) estimated from the data presented in original publication; (vii) commercial "low-temperature" MH with H storage capacity about 1 wt.%; energy storage density for the whole system (PEM+MH) of 85Wh kg^{-1}/123Wh L^{-1}; (viii) MH canisters connected in a common liquid cooling circuit with the PEMFC ("low-temperature" MH); the hydrogen storage system allowed up to 40 min of operation after each recharge; (ix) "low-temperature" MH; (x) estimated assuming stack efficiency of 0.5 and H_2 discharge rate data presented in the original publication; (xi) "low-temperature" MH; 5 canisters (HBank); (xii) MH buffer tank in the H_2 supply line from natural gas reformer; (xiii) literature data used for simulation/modelling.

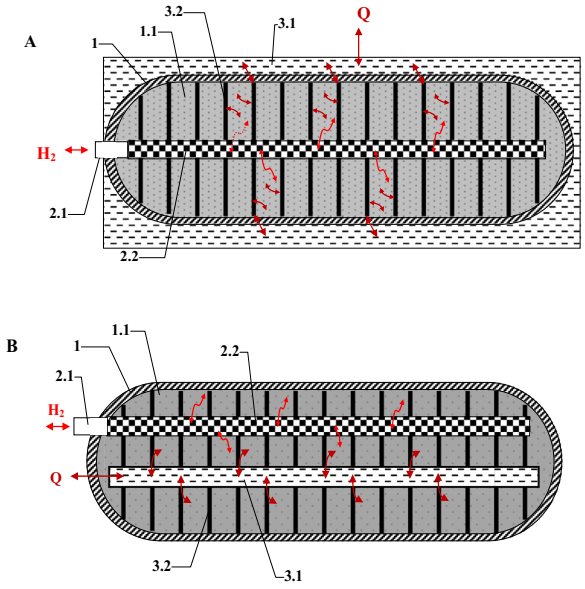

Fig. 4. Typical layouts of MH containers with external (A) and internal (B) heating / cooling: 1 – gas-proof containment, 1.1 – MH material; 2 – gas input/output and distribution system, 2.1 – H_2 inlet / outlet pipeline, 2.2 – gas filter; 3 – heat management system, 3.1 – heating / cooling means, 3.2 – heat distribution means. Adopted from ref. [28].

summarised information about MH containers and layouts of MH beds for hydrogen compression applications and on-board hydrogen storage systems for FC hydrogen vehicles can be found in the reviews by Lototskyy et. al [28] and Mazzucco et. al [116] published in 2014.

Generally, MH containers (see Fig. 4) are comprised of; a gas-proof containment (1) in which the MH material is placed, a system for H_2 input/output and its distribution within a MH bed (2), and a heat management system (3). The containment (1) isolates the MH material (1.1) and hydrogen gas from the outside environment; it also has to withstand the temperatures and pressures related to the uptake and release of hydrogen within the MH bed. The system (2), via inlet/outlet pipeline (2.1), provides H_2 supply to the MH during refuelling, or H_2 delivery from the MH to the FC stack during its operation; it also has to provide unimpeded H_2 transfer to/from external gas pipelines from/to all the points in the MH bed, as well as to prevent contamination of the external pipelines with fine particles of the MH material. As a rule, this is achieved with the help of a gas filter (2.2) penetrating through the MH bed. Finally, the heat management system (3) is intended for the removal and supply of the heat released or absorbed during refuelling (absorption) or H_2 supply to the FC (desorption) in accordance with the direct and reverse processes of Reaction 1, respectively. The heat management system (3) usually includes heating/cooling means (3.1) and means for heat distribution in the MH bed (3.2).

The main challenge in the development of MH containers is in achieving a compromise between the hydrogen storage density, integrity of the containment at the operating conditions and dynamic performance of hydrogen uptake and release. Manufacturability and lowering the costs are also very important factors to consider.

Typical geometries of MH containers, and subsequently the MH beds dispersed within them, include cylindrical (tubular) and planar (rectangular or disc-shaped) designs [113–116]. Examples are presented in Figs. 5 and 6.

Both of the geometries shown in Figs. 5 and 6 have its own advantages and drawbacks. As a rule, the planar geometry (shown in Fig. 6) is characterised by improved heat transfer performance and, accordingly, faster H_2 charge/discharge dynamics for large size MH containers. The performance can be further improved by, for example, introducing a number of heating/cooling tubes penetrating through the MH bed in the direction perpendicular to the larger plane [118]. At the same time, gas vessels with a planar geometry have low structural strength and cannot withstand high internal pressures.

MH containers with cylindrical geometries are used more frequently and can have a number of design variations. For example, hydrogen can be supplied both axially and radially to enable uniform mass transfer. The major advantage of such a system is that in order to achieve the desired system capacity, single MH units can be arranged in bundles so individual canisters can easily be replaced without disrupting the hydrogen supply to the FC [116]. Further, a multi-tubular configuration can be optimised with integrated active cooling and heating to improve H_2 uptake and discharge. Work by Krokos et al. [119] found that an increase in the number of MH tubes within the bundle resulted in an overall improvement in hydrogen storage and cooling time due to the increase in tank surface/MH volume ratio. It was also found that to improve heat management, the individual tubes should be arranged in a uniform manner in order to utilise the space containing the heating/cooling fluid more effectively.

In general, the design variations of MH containers are related to the layout of the heat management system in which the heat supply and removal is carried out either from outside (Fig. 4A) or from inside the container (Fig. 4B).

The charge/discharge of MH hydrogen storage tanks requires significant amounts of heat to be removed from/supplied to the MH material. For example, during the charge of a 0.9 kg H_2 MH tank on-board a FC forklift comprising a “low-temperature” AB_2-type MH material, (ΔH^o=−21.57 kJ (mol H_2)$^{-1}$), the amount of released heat is higher than 8 MJ [97]. Assuming a refuelling time equal to 10 min, the cooling capacity of the MH bed must be about 13 kW. Alternatively, H_2 supply from the same MH tank to a 10 kW FC stack operating at maximum power with 50% efficiency, (required H_2 supply rate 111.1 NL min^{-1}) is associated with a power required for MH heating of approximately 1.8 kW. Accordingly, the heating/cooling method of the heat management system should provide the necessary heating/cooling power associated with high heat transfer area between the MH bed and heating/cooling fluid and/or intensification of the heat transfer by e.g. using heat pipes [103,120,121]. For “high temperature” MH materials additional heating techniques may include catalytic combustors [40,121] or electric heaters [60]; some solutions use phase change materials (PCM) to provide efficient heating/cooling of the MH bed at a high temperature close to the temperature of phase transition in the PCM [122].

Furthermore, the heat supplied to or removed from the MH container should be effectively distributed in the MH bed. Taking into account the low thermal conductivity of the powdered MH materials this is a very challenging problem and solutions to ensure effective heat distribution, including augmentation of the heat transfer within the MH bed, are of paramount importance [29]. Commonly used solutions include the introduction of heat-conductive matrices such as heat-conductive metal foam [123,124], transverse or longitudinal fins [53,113,125] or complex wire configurations [126] within in the MH bed. Heat distribution in the MH can also be improved by making porous hydride compacts where the binder is a metal [127,128] or recompressed Expanded Natural Graphite (ENG) [129,130]. Porous powder metal – MH compacts coated with copper were shown to have very good heat transfer augmentation and to be strong enough to remain intact for over 3000 absorption/desorption cycles [131].

Table 3 summarises typical layouts of the heating/cooling and heat distribution accessories used in cylindrical MH containers mainly intended for hydrogen storage and its supply in FC systems. From Table 3 it can be seen that the heating and cooling of MH containers can be managed either from the outside or by introducing various heating/cooling structures (mainly liquid heated/cooled heat exchangers) in the MH bed. In both cases, long MH tanks with a smaller diameter are preferred due to a shorter heat transfer distance and better heat dissipation in comparison to wider tanks. Some layouts use combined (external + internal) heating and cooling; this is particularly

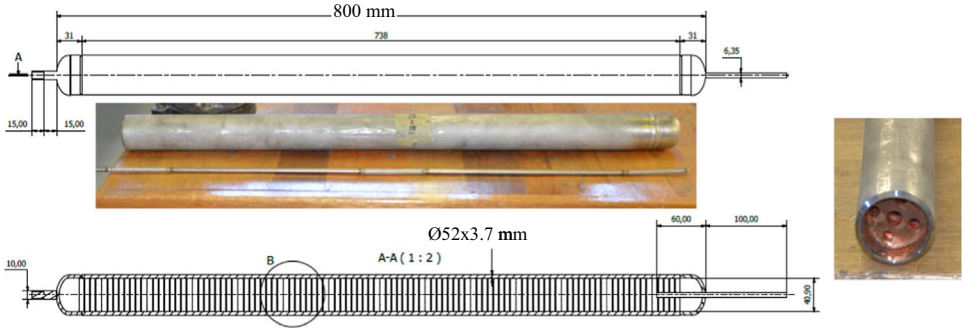

Fig. 5. Disassembled view and schematic drawing of cylindrical MH container with external heating/cooling developed by HySA Systems (South Africa) [44].

effective when fast heating or cooling of large MH containers is necessary [147].

In the case of external convective heating and cooling with low surface heat transfer coefficients (e.g. when air is used as a heating/cooling fluid), the heat transfer can be intensified further by increasing the heat exchange area (e.g. external finning). As a rule, the heat distribution in MH beds dispersed in externally heated/cooled MH containers is provided by the use of heat conductive fins within MH powder, or in combination with other methods for the augmentation of heat transfer specified above (metal foam, compacts). In MH containers with internal heat supply and removal, the heat distribution means form part of a heat exchanger disposed in the MH; in addition to the above-mentioned solutions (fins, compacts, etc.), various designs of heat exchangers with increased heat exchange areas and reduced heat transfer distance (e.g. tube bundle or coiled tube) can be used.

The efficiency of the heat distribution first of all depends on the size of the MH container and operating conditions. For small systems with a H_2 storage capacity of tens of NL H_2 and FC power up to tens of W, normal operation takes place even without heat transfer augmentation. However, when the unit size and FC power increases, insufficient heat distribution in the MH bed results in a limitation of the H_2 supply and, accordingly, a decrease in the amount of H_2 which can be supplied to the FC stack operating at a specified power. This effect is illustrated in Fig. 7, adapted from ref. [43], in which the performances of MH containers for FC applications made according to various layouts (##1–6, see Table 3) were compared experimentally. It can be seen that the useable amount of hydrogen (in % of the maximum hydrogen storage capacity of MH container) drops with the increase of the FC power divided by the amount of MH in the container. Improved performance of the heating/cooling and heat distribution systems in the container results in a smaller drop and, accordingly, more complete utilisation of hydrogen stored in the MH occurs at higher FC power.

Many of the developments reported above included modelling of heat transfer performances of the MH beds [53,68,108,119,125,132,136–139,148–150]. A review of the modelling activities aimed at the optimisation of dynamic performances of MH reactors for hydrogen storage applications has been recently published by Mohammadshahi et al. [150]. Although effective modelling still requires experimental validation and calculations are often based on assumptions, it is a useful tool for predicting the behaviour of MH's during hydrogen uptake and discharge and how it is influenced by factors including flow rate, temperature and hydrogen concentration distribution. For practical applications, modelling enables the user to find an optimal design of the heating/cooling and heat distribution systems of a MH container of a given geometry and size. Prediction of the dynamic charge/discharge performances, which depend on the bed geometry and size as well as the pressure-temperature operating conditions, is particularly important. For example, ref. [132] provided a comparative performance analysis of cylindrical MH beds comprising the same powder of AB_5-type MH material and having same size (ø60×500 mm). The considered layouts included; (i) internal cooling/axial heat exchange tube, (ii) internal cooling/coiled heat exchange tube, (iii) external cooling without heat transfer augmentation in the MH, and (iv) external cooling/transversal heat distribution fins (pitch 5 mm). It was shown that the layouts (iv) and (ii) exhibited the best dynamic performances of hydrogen uptake. Additional advantages of the layout (iv) included simplicity and lower costs, as well as a less pronounced reduction of the hydrogen storage capacity using the same MH bed dimensions.

The design of MH containers filled with MH powder should anticipate careful alignment of the MH filling density. On one hand, more dense packing of the MH in the containment increases the

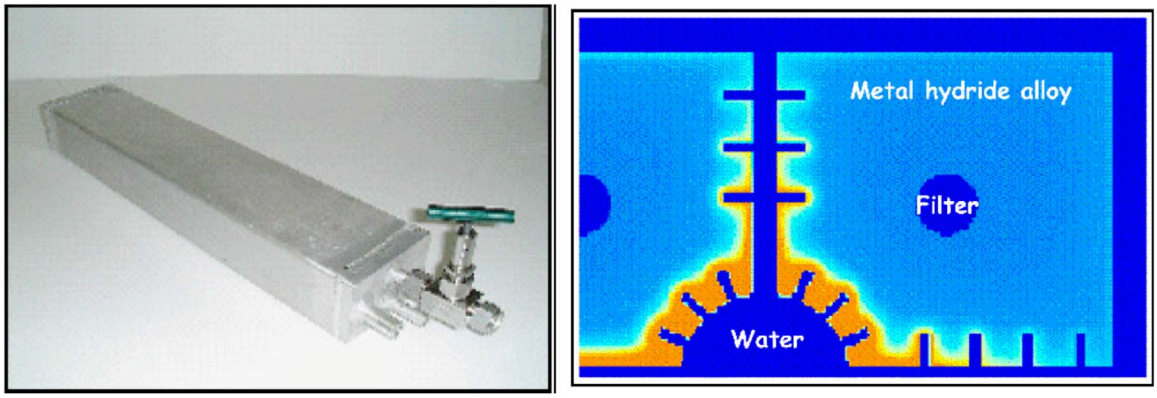

Fig. 6. General view (left) and computer-generated cross section (right) of rectangular MH container with internal heating/cooling developed by Japan Metals and Chemicals, Inc. (Japan–USA) [117].

Table 3
Layouts of the heating/cooling and the heat distribution means in MH containers.

Heating/cooling	Heat distribution in the MH	References	Ref. ## (Fig. 7) / H storage capacity [NL]
External / flat surface	Powdered bed (no augmentation)	[43,53,68,86,108,125,132]	1/10
	Powdered bed with fins	[43,44,57,68,97,132,133]	2[a] /90; 3[b] /90
	MH powder in metal foam	[84]	
	MH powder in metal foam with fins	[134]	
	MH/ENG compacts with fins	[122,135]	
External / finned surface	Powdered bed (no augmentation)	[53,120,125]	
	Powdered bed with fins	[43,81,133]	5[b,c] / 700
	MH/ENG compacts with fins	[43]	4[b] / 90
Internal	Straight tube in powdered bed	[53,125,132]	
	Tube bundle in powdered bed	[68,136]	
	Coiled tube in powdered bed	[91,132,137,138]	7 / 6350
	Straight finned tube(s) in powdered bed	[43,67,68,90,121,125]	6[d] / 1900
	U-tube with fins in powdered bed	[77,94,99,104,137,139]	
	Finned coiled tube in powdered bed	[138]	
	Tube penetrating through MH powder in metal sponge	[140]	
	Tube penetrating through MH/metal compact	[141]	
	Finned tube(s) in MH/ENG compacts	[60,142]	
Internal / composite (hybrid) containment	Powdered bed in cassette with heat exchanger structure	[38,107,143–146]	
Combined	External jacket + internal straight tube	[55]	
	External jacket + internal tube bundle	[136]	

Notes:
[a] transversal copper fins pressed in the container, pitch 5 mm
[b] transversal aluminium fins inserted in the container, pitch 5 mm
[c] longitudinal aluminium fins pressed in the container, pitch 15 mm
[d] transversal copper fins pressed on the core tube, pitch 10 mm

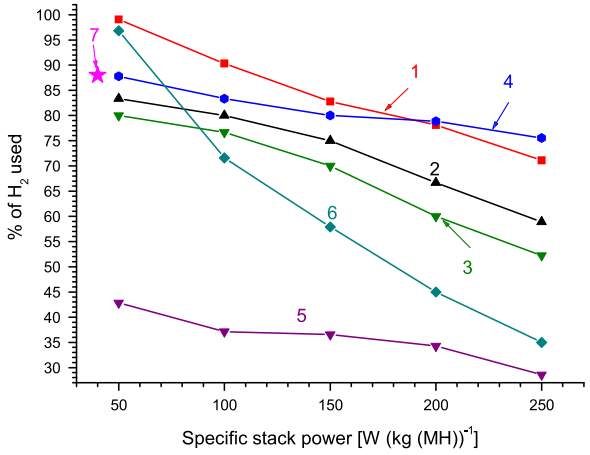

Fig. 7. Amounts of hydrogen supplied from different MH containers providing stable operation of a LT PEMFC stack having an efficiency of 50% [43]. The labels correspond to the layouts listed in Table 3. Heating conditions: 1–5 – natural convection of ambient air (T_0=20 °C), 6 – water circulation (0.5 kg min^{-1}, T_0=30 °C). The star (7) represents performance of liquid heated-cooled MH system (50 kg MH, 2 kW FC power) reported in [91].

hydrogen storage capacity on the system level [24] and the effective thermal conductivity of the MH bed [151]. However, lattice expansion during hydrogenation results in the swelling of the MH powder so if free space is not provided to allow for this, large stresses can occur on the containment wall. It has been shown that an increase of packing fraction of a $LaNi_{4.55}Al_{0.45}$ alloy in a reaction vessel (bed size ø16×75 mm) from 45 to 50 vol% results in the appearance of significant surface stress, increasing with the cycle number and reaching 250 MPa on the 100th hydrogen absorption cycle [152]. Particularly strong stresses were shown to be formed in agglomerated regions where the value of the local packing ratio increases to ~0.6; pulverisation of the MH particles during cyclic H absorption/desorption results in their concentration in the bottom part of the vessel that creates the agglomeration regions and stress generation even if the overall packing fraction is lower than the critical value [153]. The effect of MH densification at the bottom of MH container, resulting in the stress generation, can be observed even during the first hydrogen absorption cycle. This was shown in ref [91] in a large MH container[2] where the stress value reached 91.9 MPa during the first absorption. The stresses can cause significant deformations or rupture of the containment as illustrated in [28].

"Hybrid" hydrogen storage containers, in which the MH material (with low hydride thermal stability) is placed in high pressure composite cylinders, thus combining compressed hydrogen gas (CGH2) and MH hydrogen storage options, is a very promising solution. It allows for a significant increase in the volumetric hydrogen storage capacity and decrease in storage pressure (in comparison to CGH2 storage), as well as an increase in flow rate of H_2 delivered to the FC and shortened refuelling time (in comparison to MH storage). The performances of hybrid hydrogen storage tanks were presented in detail in a number of publications [38,107,143–146]; the corresponding developments related to hydrogen storage for on-board FC vehicles are actively carried out by Toyota and other vehicle manufacturers. The advantages of hybrid hydrogen storage appear at quite low fraction of hydrogen stored in MH: the recommended volume ratio of the MH to the total system is between 3% and 30% [154–156]. The main disadvantage of hybrid hydrogen storage tanks is their high cost. This is mainly associated with the use of expensive high-pressure composite cylinders which require leak-proof and pressure-rated fittings for the input/output of the heat transfer fluid to/from the high pressure containment. Further, high charge pressures, $P \geq 350$ bar, are the origin of the high indirect costs associated with the use of expensive refuelling infrastructure similar to the one for CGH2 fuel systems.

[2] Inner diameter 155.2mm, length 1m; coiled internal heat exchanger, tube diameter 25.4mm, overall length 19.7m. The container was loaded with 50kg of the $MmNi_5$ powder that corresponds to filling density of 3.04gcm^{-3}, or 45.4% of the material density in the hydrogenated state

3.3. General layouts of fuel cell and metal hydride integrated systems

The integration of MH's with FC's mainly relates to their thermal coupling. As a rule, it realises the concept schematically shown in Fig. 2 in which part of the heat released during the FC operation is directed to the heating sub-system of MH containers. There does, however, exist some exceptions to this rule. For example, at low FC power - associated with low H_2 consumption and the use of a MH material characterised by H_2 equilibrium pressures at ambient temperature higher than it is necessary for the H_2 supply to the FC - the heat absorbed by the MH from the environment can be sufficient to provide H_2 desorption and special thermal management is not required [43,86]. Conversely, when the amount of heat released during FC operation or temperature potential of the heat is insufficient for the decomposition of the MH (see Section 2), heating of the MH tank is assisted by electrical heaters [61], or by catalytic combustion of part of the hydrogen supplied to the FC [48].

In most cases, thermal integration of MH tanks with liquid-cooled FC's is provided by an extension of the stack cooling loop, which includes additional heating accessories for the MH containers [48,57,63,65,77,80,95,98–101,104,157]. The stack coolant (T=60–80 °C for LT PEMFC) is directed to heat exchangers which are either embedded in the MH containers (Fig. 4), or form part of specially designed thermal holders [57]. This solution is efficient, however, it must only use special ultra-pure heat transfer liquids suitable for the safe cooling of the FC stacks. It also poses strict requirements to the piping of the MH heating sub-system to avoid contamination of the liquid.

Direct thermal coupling of MH's and FC stacks using heat pipes was described in ref. [103]. For high-temperature applications (e.g., when MgH_2 is used to supply hydrogen to SOFC), the heating of the MH bed can be provided by exhaust gases from the FC stack [59]. In the developed system, the heat released from a 1 kW SOFC during operation (~750–800 °C) was sufficient to desorb the hydrogen from the MgH_2 tank, which has a specific heat requirement of 75 kJ (mol H_2)$^{-1}$. Overall, it was found that thermal integration of the MH tank with the SOFC is possible but requires careful consideration of the thermal management of the system.

For air-cooled PEMFC stacks, the MH containers can be heated directly by the exhaust warm air [43,158]. Alternatively, the MH containers can be heated by a separate loop of circulating liquid which includes heat exchangers, heated by the exhaust air [38,44,53,55,67,97,102]; this solution could be used for both air- and liquid-cooled stacks. In the latter case, a secondary circulating loop of the heating liquid thermally coupled with the stack cooling system can be used as well [54,83]. The MH thermal management sub-system can also be integrated in thermal loops of the whole FC power system, like CHP [106] or hydrogen fuelled vehicle [159]; in addition to MH heating from the heat-releasing system components, these solutions can foresee an additional thermal loop for MH cooling during refuelling [159].

The solutions described in the previous paragraph use indirect thermal coupling of MH's with FC's that may be associated with a loss of the heat transfer efficiency. However, taking into account the fact that the use of “low-temperature” MH's for the hydrogen supply requires only a minor part of the heat released during FC operation (see Section 2), we consider these solutions as promising from a practical viewpoint due to their simplicity and flexibility.

In most cases, hydrogen supply from a MH tank to a FC stack uses straightforward solutions in which the gas manifold of the tank is connected to the hydrogen input valve of the stack via a pressure reducer. The tank gas manifold can also be connected to the hydrogen supply line for refuelling. Alternatively, it is possible to quickly replace used MH tanks with the charged ones [54,57]. In some cases the gas manifold of the MH tank is connected with the pipeline for H_2 supply to the FC stack via gas buffer, to provide quick start-up of the FC [48], and/or to smoothen H_2 pressure fluctuations during the operation [55].

Very effective system integration solutions can be achieved by using a combination of some of the features specified above. For example, a combination of: (a) low thermal stability MH's conventionally used in “hybrid” hydrogen storage containers, (b) indirect thermal coupling of the FC stack and other system components releasing heat during the operation with the MH thermal loop, and, (c) installing a CGH2 buffer on the MH tank gas manifold, resulted in the development of a highly efficient “distributed hybrid” CGH2+MH hydrogen storage system [67,160]. This configuration has been successfully demonstrated in a FC forklift with hydrogen storage MH extension tank [44,97].

4. Integrated metal hydride and fuel cell power systems

Hydrogen storage solutions based on MH tanks have been implemented and demonstrated in various FC powered systems including; portable applications [158,161–163], light FC vehicles [57,64,67,69,79,95,98], FC forklifts [44,63,97] and underground mining vehicles [54,75], and various stationary systems based on LT- [38,61,82,83,164–166] and HT- [77] PEMFC, as well as SOFC [59].

Modelling, simulation and design are important steps which must take place before assembling and testing of the final MH – FC system can be carried out. For this reason, although they do not include the making and characterisation of the integrated systems, articles dealing with the above mentioned topics [31,65,78,80,85,90,106,157,167–174] are crucial for developing proper system engineering solutions. Modelling activities have focused on various aspects of the dynamics of thermal and mass balance in systems where MH's have been integrated with PEMFC [31,65,78,80,85,90,106,157,167,168,171,173] and SOFC [169,170]. In some systems, additional integration of an alkaline or PEM electrolyser has been considered [31,106,167]; refs [85,174] consider unified PEM electrolyser – FC units (regenerative fuel cells). In addition to hydrogen storage applications, some modelling works [78,170,171] consider the use of MH's for heat management solutions (e.g., air conditioning units).

Nevertheless, the practical implementations of MH – FC system integration is the most interesting part of the topic covered by this review. Some specific examples will be given below.

4.1. Portable applications

As a rule, portable applications involving MH + FC power systems use open cathode air cooled LT PEMFCs (x1–100 W in electric power) and are characterised by simple solutions for the integration of a FC and MH hydrogen storage system of a modest (x10–100 NL H_2) hydrogen capacity.

Fernández-Moreno et al. [161] built and tested a portable power system based on single air-breathing PEM FC and commercial MH cartridge from Horizon with a capacity of 1 g H_2. The built-in DC-DC converts low voltage (0.5–0.8 V) and high current output (200–300 mA cm^{-2}) into 3.3 VDC in order to power electronic applications. The power system was able to provide 1 W of electricity to an external application for 20 h by using one charged MH cartridge. It was demonstrated that one air breathing PEM FC can provide high enough energy densities and autonomy for portable applications.

Air-breathing FC systems have been demonstrated as a replacement to Li-ion batteries in mobile phones [163]. The system was integrated at the back of the phone together with an AB_5 MH hydrogen storage tank (4 NL H_2). The energy storage density of the complete system was found to be 205 Wh L^{-1}.

A FC powered portable freezer with an air cooled MH canister was presented in ref [162]. In the developed system a 300 W air cooled PEM FC stack was fuelled from commercially available hydride canisters provided by Ovonic [165,166], while generated heat from the stack was used for hydrogen desorption. The minimum achieved

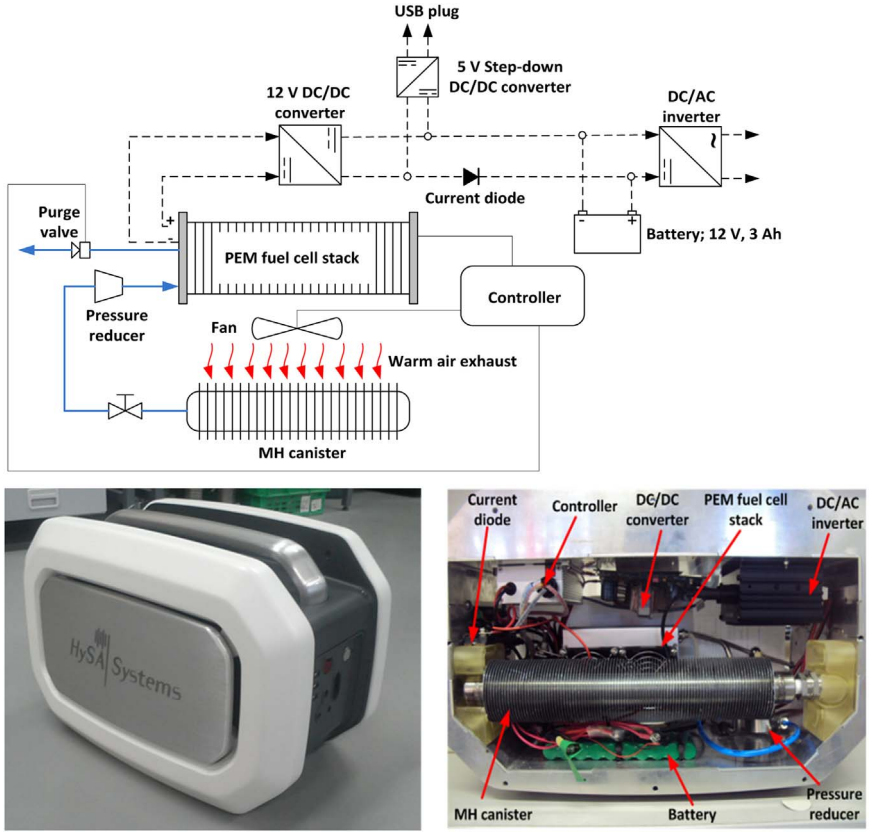

Fig. 8. Schematic layout (top) and general view (bottom) of the LT-PEMFC portable power system developed by HySA Systems [158].

cabinet temperature of the freezer was −21.8 °C, at an ambient temperature of 26.6 °C, while the maximum system efficiency was found to be 37% (based on the lower hydrogen heating value, *LHV*).

A LT-PEMFC system rated for a maximum output power of 130 W with 240VAC and 5VDC USB electric outputs (Fig. 8) was developed by HySA Systems / South Africa [43,158]. In the system, hydrogen is supplied from a 90 NL H_2 MH canister which uses a multi-component AB_2-type hydrogen storage alloy and has enhanced heat transfer performances achieved through a combination of MH/ENG compacts with internal and external finning of the MH container. The MH canister allowed for > 40 min stable operation at the maximum stack power with the utilisation of > 90% of the stored H_2.

An overview of the development of replaceable MH containers (MH cartridges) for small-scale (< 1 kW) FC applications has been recently presented by Iosub et al. [175]. In these canisters hydrogen is stored in composites embedded in the cartridges, comprising MH's with additives of a polymer binder and a component (graphite, copper or aluminium) which improves heat transfer performance.

4.2. Mobile applications

Fuel cells represent a promising market niche in a number of mobile applications. Although battery electric vehicles (BEV's) are superior for shorter ranges (i.e., city driving) because batteries have better roundtrip (charging-discharging) efficiency than regenerative FC's, in passenger vehicles, FC's offer better volumetric energy density than the battery systems, resulting in longer driving range, comparable to today's internal combustion fuel vehicles. Another advantage of fuel cell electric vehicles (FCV's) over BEV's is the short refuelling time which is comparable to today's diesel and gasoline vehicles. In FCV's hydrogen is usually stored on board in 350–700 bar compressed gas composite cylinders which can achieve storage density of above 3% by weight. Such a storage density cannot be achieved by MH systems alone, however, they have a number of advantages in light FCV's where the required amount of H_2 fuel stored on board is not very big. Further, in certain mobile applications, including material handling vehicles (see Section 4.2.2), the high weight of the MH systems becomes advantageous.

An overview of the applications of MH in various FCV systems is presented below.

4.2.1. Light fuel cell vehicles

Currently, light electric vehicles (LEV) powered by FC's are one of the most commonly targeted applications in the implementations of FC – MH systems. The features of some developments are described below.

A hybrid energy system comprising 1.5 kW PEM FC (MES-DEA SA / Switzerland), battery pack, ultra capacitor and 1 Nm^3 H_2 MH storage tank was presented in ref. [79]. The MH tank is based on MHS-1000IHE MH containers (Treibacher Industrie AG / Austria) equipped with internal heat exchangers and uses AUERSTORE AB_2-type MH alloy. The system was integrated in a wheelchair, and the overall system efficiency was found to be higher than 36%.

A PEM FC – lithium ion battery hybrid scooter was developed by Shih et al. [69]. The system comprises of an air-cooled self-humidified 2.3 kW PEM FC stack, lithium-ion battery, five low pressure MH canisters (HBank / Taiwan; H_2 capacity 220 NL each) arranged in series, quick connector, DC/DC converter and an electronic control unit. The exhaust air from the FC is utilised to heat the MH canisters during H_2 desorption. The maximum scooter speed is 53.2 km h^{-1}, with a distance of 63.5 km between H_2 refuelling. It was concluded that further system improvements are needed to extend the scooter range.

A hybrid power system for a LEV equipped with a liquid cooled PEM FC, lithium-ion battery and liquid heated aluminium MH hydrogen storage canister filled with an AB_5-type alloy was built and tested by Hwang and Chang [57]. The MH system was thermally

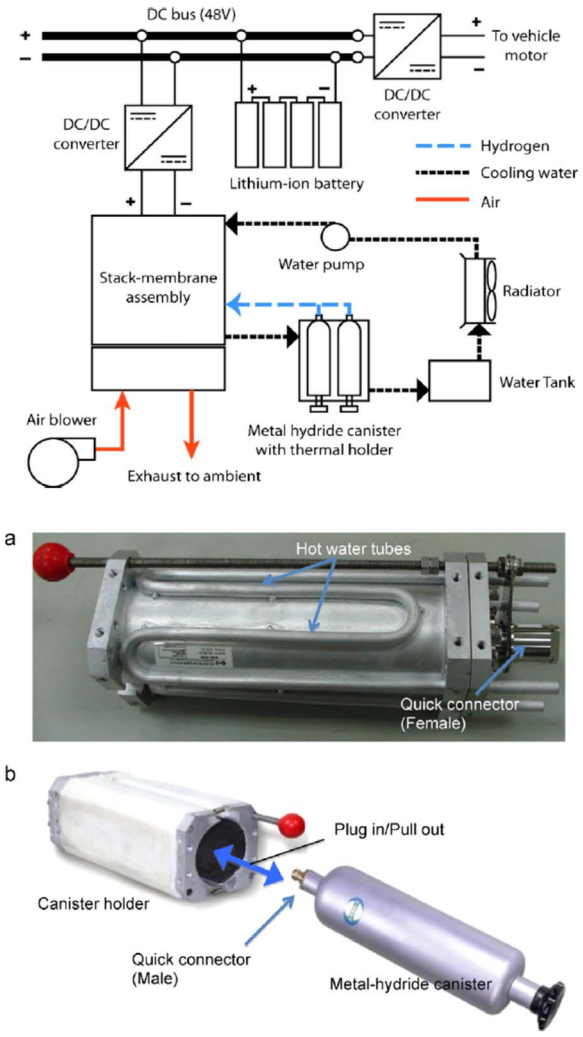

Fig. 9. Hybrid power system for LEV. Top – system layout. Mid (a) – thermal holder of the MH canister. Bottom (b) – assembly of the MH canister and the holder. Adopted from [57].

coupled with the FC stack cooling loop using an original design solution (thermal holder; see Fig. 9) which allowed replacement of a depleted canister with a charged one in only 1–2 min. The H_2 storage capacity of one canister was ~45 g with a recommended charging pressure of ~10 bar. One fully charged MH canister was found to provide a H_2 flow rate of 8.2 SLPM for 55 min. The maximum efficiency of the hybrid power system was reported to be 46% due to the use of a new generation FC stack and recovery of the waste heat for H_2 desorption.

Another example of a thermally coupled FC stack with a MH tank and its integration into a three wheeled tourist LEV as range extender was disclosed in ref [64]. The hydrogen capacity of the MH tank was 1500 NL.

The development of a hybrid PEM FC powered system and its integration into a mini train, with a capacity of 9–12 persons, is presented in [95]. The system uses hydrogen from four low-pressure liquid cooled MH hydrogen storage tanks which are thermally coupled with the FC stack cooling loop. The MH hydrogen storage tank uses an AB_5-type alloy and has a capacity of 44.8 g H_2 with an availability of 93%.

A FC powered LEV (John Deere Gator™) with an integrated FC power module was developed by Fuchs et al. [98]. The FC stack (Energy Partners [98]) has an output power of 8.3 kW and operating pressure of 150 kPa and uses hydrogen from two MH hydrogen storage tanks from Westinghouse Savannah River Co. The MH material (FeTiMn) provides a discharge pressure of 756 kPa (7.56 bar) at T=50 °C. The

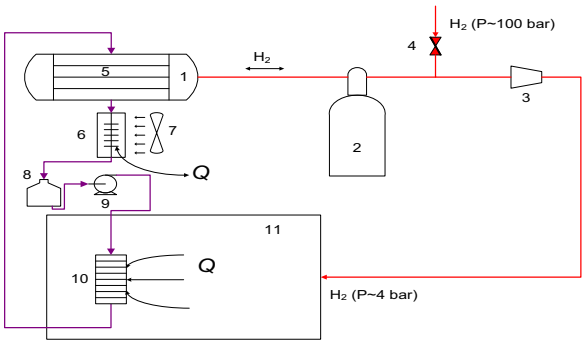

Fig. 10. Layout of the "distributed hybrid" hydrogen storage and supply system integrated in electric golf cart with fuel cell range extender. 1 – MH container; 2 – CGH2 buffer; 3 – pressure reducer; 4 – H_2 recharge valve; 5 – heat exchanger of the MH container; 6 and 10 – air–liquid heat exchangers; 7 – fan; 8 –expansion tank; 9 – circulation pump; 11 – fuel cell stack (FCgen-1020ACS in Nexa® 1200 power unit). Adopted from [67].

total H_2 capacity is close to 2 kg, and the fuel-to-storage system weight ratio approaches 1%. The H_2 storage system allows seven hours operation between hydrogen refuelling.

In 2013 authors of the review (IT, ML) reported the development of Africa's first electric golf cart with a FC range extender [176]. The vehicle was later equipped with a "distributed hybrid" hydrogen storage and supply system comprising a liquid cooled/heated MH tank thermally coupled with the FC and other heat – generating BoP components [67]; see Fig. 10. Driving tests on the golf cart revealed significant prolongation of the driving time from 1.5 h with separate CGH2 or MH storage, to 5 h with combined CGH2 and MH storage; in all the cases the H_2 refuelling pressure was about 100 bar.

4.2.2. *Marine applications*

Along with ground LEV, boats may also be an interesting niche market for FC systems. Clean and quiet operation of FC boats is particularly appealing for their use in national parks. A 1.2 kW fuel cell power system (Nexa / Ballard) was used by Barbir et al. [177] to power a small boat equipped with a 600 W electric outboard motor (M26 E-Drive by Yamaha). A DC/DC converter/voltage regulator was used to match the voltage of the motor (12 V). Two 12 V 65 Ah batteries were incorporated in the system in order to provide 24 V required for the Nexa system start-up, but they also provided additional energy. Hydrogen was stored in 3 MH bottles; each 2.6 l bottle contained up to 600 NL H_2 at 10–14 bars. This configuration was able to run the boat at the speed of 4 knots for more than 5 h (3 h of running time coming from stored hydrogen and 2 h from the batteries).

Another example of a marine application involving a FC thermally coupled with a MH tank was shown by Bevan et al., [178] who developed a hydrogen powered canal boat which operates using a combination of a MH hydrogen storage tank ($TiMn_2$ type alloy) with a total storage capacity of 4 kg H_2, PEM FC, lead-acid battery pack and a high-efficiency permanent magnet (NdFeB) motor. In the system, the FC was integrated as a range extender (typical solution for LEV's; see [176] and references therein) that allowed the developers to use quite low power (1 kW) PEM FC stack when the motor power can be as high as 4–5 kW.

Intermetallic hydrides were also considered as a viable hydrogen storage option for auxiliary (~10 kW_e) and megawatt-scale main power (modules up to 250 kW_e) on board ship fuel cell power plants [179].

Fiori et al., [180] reviewed a range of MH materials suitable for use in LT-PEMFC submarine applications with the ultimate aim of increasing the storage capacity and subsequent autonomy (air independent propulsion) of the vessel. The requirements for such a MH material included; a storage capacity of 120 g dm^{-3}, operating temperature of 20–50 °C, desorption pressure of 2–3 bar H_2 and cycle life of at least 150 charge/discharge cycles to ensure operation over a 30

year period (with an average of 5 cycles per year). After reviewing several different classes of MH, ranging from simple binary compounds such as FeTi to materials based on TiZrMnVCu, the authors concluded that solid solution metallic hydrides offer the most promise for submarine applications. Further, the low desorption pressures that these alloys often experience can be overcome by doping the MH with a suitable material (e.g. Ti or Si).

4.2.3. Heavy duty fuel cell utility vehicles

The use of FC's in heavy duty utility vehicles, including material handling units / forklifts, has a number of advantages over similar battery-driven vehicles. Fuel cell powered forklifts have constant power during the entire shift while the battery powered ones lose speed over the last half of the battery charge. The H_2 refuelling time for FC forklifts is much shorter than the time necessary for the battery recharge in battery-driven forklifts; 1–3 min vs. ~8 h. To provide uninterrupted operation of the latter, 2–3 batteries are needed per one forklift; one battery installed on-board, one charging and one on cooling. The battery swapping is time consuming (~20 min), and there is an issue of personnel safety during replacement the heavy (~2 t) battery. The use of FC's eliminates the necessity for additional warehouse space, as well as the costs for handling and storing toxic materials associated with the intensive operation of battery driven forklifts.

The application of MH's in FC powered forklifts and underground mining vehicles is especially promising. Proper counterbalancing of these vehicles requires additional ballast which can be provided by the use of "low-temperature" intermetallic hydrides with hydrogen storage capacities below 2 wt% (i.e. storage of 1 kg H requires more than 50 kg of the MH material). The use of MH "ballast" could result in the increase of the amount of stored H_2 at the same unit size. Thus, the low weight capacity of intermetallic hydrides, which is usually considered as a major disadvantage to their use in vehicular hydrogen storage applications, is an advantage for the heavy duty utility vehicles considered in this section [97].

A FC hybrid power source for an electric forklift was developed by Keränen et al. [63]. The system consists of a PEM FC stack (16 kW), ultra capacitor modules and lead-acid battery. Hydrogen was stored in MH canisters connected to a common liquid cooling circuit with the FC allowing up to 40 min of operation after each refuelling. This concept also offers additional cooling of the FC system during hydrogen desorption from the MH canisters.

Lototskyy et al. [44,97] integrated a commercially available LT PEMFC power module (Plug Power / USA) into an electric forklift (STILL / Germany). In this system (see Fig. 11), a MH extension tank was thermally coupled with the stack cooling system via an air-to-liquid heat exchanger. The MH tank uses an AB_2-type MH characterised by H_2 equilibrium pressure above 10 bar at room temperature and comprises an advanced MH bed which provides easy activation and fast H_2 charge/discharge. The system has the same useable hydrogen storage capacity (~19 Nm^3 H_2 or 1.7 kg) as the separate CGH2 tank charged at P=350 bar, but at a significantly lower H_2 charge pressure (185 bar). This work also presents a hydrogen refuelling station (dispensing pressure up to 185 bar) with integrated MH compressor developed for the forklift refuelling. Heavy duty tests according to VDI2198 (VDI-60 cycle) protocol and light duty tests of the forklift in a real industry environment showed that the energy consumption was 9.56 kWh h^{-1} and 3.87 kWh h^{-1}, respectively, with the refuelling time as short as 15 min (83% of the maximum capacity during 6 min refuelling).

Successful demonstration of a PEM FC powered mine locomotive fuelled by hydrogen from a MH tank is presented in ref [54]. In the work a commercially available 4 t battery-powered locomotive was converted into FC operated system by replacing lead-acid batteries with a PEM FC (Nuvera Fuel Cells Europe) and MH H_2 storage system (Sandia National Laboratories / USA) comprising 213 kg of Hydralloy C15 AB_2-type alloy from GfE / Germany. The total hydrogen storage capacity is 3 kg which is sufficient for 8 h of the locomotive operation.

Integration of the FC and MH system into a 10 t fuel cell powered mine locomotive and mining dozer was demonstrated by Anglo American Platinum Ltd. in ref. [75]. Both systems use liquid-cooled LT PEMFC stacks (velocity-9SSL V4; Ballard / Canada), with a continuous net electric power of 9 kW and 17 kW for the dozer and the locomotive, respectively. The latter system uses a liquid cooled/heated MH hydrogen storage tank with a rated capacity of 3.5 kg H_2. The system performance generally matches the design specification, except for shorter operation time (3.5 against 8 h) which can be explained by incomplete refuelling at the operating conditions (10–15 bar H_2, cooling by mine water or ambient mine air).

4.3. Stationary applications

Most hydrogen FC power systems (≥1 kWe) for stationary and non-vehicular mobile applications are not strictly limited by the system weight but frequently pose limitations as to their footprint which makes it promising to use MH for the compact hydrogen storage.

Ref. [38] presents work on a FC mobile light tower which incorporates a 5 kW FC stack from Altergy Systems, Grote Trilliant LED lighting and a MH hydrogen storage (3 kg H_2 /190 kg in total 2.7FW1104 tank which uses OV679 Ovonic interstitial MH alloy). The FC stack is cooled by ambient air, and the dissipated heat is utilised in an air-to-liquid heat exchanger to intensify H_2 desorption from the MH. It was found that hydrogen refuelling is possible even without an external source of cooling water, by only using existing BoP components of the stack thermal management. The hydrogen refuelling takes between 3–8 h, while in the case of external cooling by chilled water rapid recharge is possible in ~20 min. Overall, it was shown that it is technically feasible, and in some cases beneficial, to use MH storage in FC lightning equipment but for commercialisation the cost of the MH H_2 storage technology still needs to be reduced.

Gonzatti et al. [164] reported developments and testing of a prototype integrated power plant using a LT PEMFC stack (GreenHub-3000, 3 kWe in the nominal power; Horizon Fuel Cells Technologies), alkaline electrolyser (HP model, up to 6.67 NL min^{-1} H_2 at P≤15 bar; Piel-McPhy Energy) and MH hydrogen storage. The MH cylinder used in this development was the HBOND-7000 L model manufactured by LabTech (46 kg of (LaCe)Ni_5, 7140 NL hydrogen storage capacity, H_2 delivery at P=2–10 bar and T=10–30 °C). The tests demonstrated an overall efficiency of about 11% due to the low efficiencies of the commercial electrolysers and power inverters used in the experiments.

A hydrogen based auxiliary power unit (APU) was presented by Doucet et al. in [82]. During day time operation, hydrogen is produced in a PEM electrolyser powered from PV arrays and stored in MH tanks comprising $LaNi_5$; the total capacity is about 1Nm^3. During night hours hydrogen is used in the PEM FC (1 kWe) for the co-generation of heat and electricity. The developed system has a high potential to be used as a power source for domestic applications.

A power system for stationary applications which incorporates a liquid-cooled PEM FC stack and MH hydrogen storage tank with commercially available $LaNi_{4.8}Al_{0.2}$ is presented in [83]. The MH tank is made of stainless steel and comprises cooper fins for the improvement of heat transfer between the stack cooling fluid and the tank. The system is able to operate for 6 h at an average power of 0.76 kW and it can deliver 4.8 kWh with a H_2 consumption of 3120 NL.

In March 2016 Toshiba Corporation announced the launch of the H2One™ hydrogen based autonomous energy supply system, which integrates renewable energy generation and uses hydrogen as a fuel for power generation [181]. This integrated system, comprising 62 kW photovoltaic panels, an electrolyser and a 54 kW FC generator, has entered operation in the Phase-2 building of the Henn na Hotel, at the Huis Ten Bosch theme park in Nagasaki, Kyushu / Japan. The system

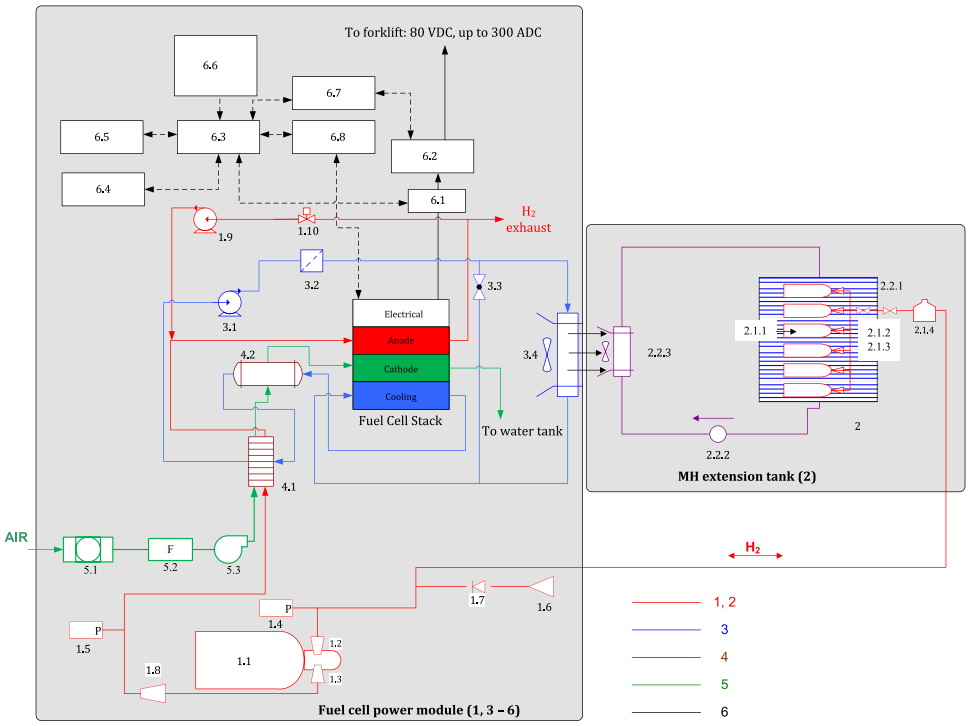

Fig. 11. Integration of a MH hydrogen storage extension tank in FC forklift [97]. 1 – hydrogen storage and supply subsystem: 1.1 – gas cylinder, 1.2, 1.3 – adapters, 1.4, 1.5 – pressure sensors, 1.6 – refuelling receptacle, 1.7 – check valve, 1.8 – reducer, 1.9 – recirculation pump, 1.10 – purge valve. 2 – MH extension tank: 2.1 – hydrogen subsystem: 2.1.1 – MH containers, 2.1.2, 2.1.3 – shut-off valves, 2.1.4 – gas filter; 2.2 – thermal management subsystem: 2.2.1 – water tank, 2.2.2 – circulation pump, 2.2.3 – radiator. 3 – FC stack cooling subsystem: 3.1 – coolant pump, 3.2 – DI filter, 3.3 – bypass valve, 3.4 – radiator. 4 – fuel / oxidant conditioning: 4.1 – reactants conditioner, 4.2 – humidifier assembly. 5 – air supply subsystem: 5.1 – filter, 5.2 – flow meter, 5.3 – compressor. 6 – electrical components: 6.1 – contactor, 6.2 – Li-ion battery, 6.3 – system master controller, 6.4 – compressor motor controller, 6.5 – cell voltage monitor, 6.6 – BoP sensors (H_2, tilt, coolant temperature, oxidant and fuel temperatures), 6.7 – battery sensors (voltage, current, SoC), 6.8 – stack sensors (voltage, current, temperature).

provides 24/7 uninterrupted supply of electricity and hot water to the hotel. Hydrogen is stored in a MH tank which is less than one-tenth the size of the conventional model it replaces; the details of the MH tank system integration have been recently reported [182].

Community hydrogen storage system including a PEM electrolyser, MH tank and PEM FC was designed, evaluated and tested in [61]. The MH tank (capacity of up to 4 kg H_2 using a MgH_2-based hydrogen storage material) was manufactured by McPhy Energy. The tank was designed for pressures up to 12 bar and temperatures up to 390 °C, and absorbed and released heat is managed using a phase change material (PCM). It was found that the system has good flexibility and capability, with a round trip efficiency of 52%.

A HT PEMFC system with integrated hydrogen storage tank based on $NaAlH_4$ is presented in [77]. The FC and MH tank are thermally coupled to utilise heat generated by the FC for hydrogen desorption. The MH tank contains 2676 g of $NaAlH_4$ doped with 4 mol.% of $TiCl_3$. In the system, around 60 g of hydrogen can be released in 3 h, which corresponds to a total stack output of 660 Wh.

MH's are also used in combined heat and power systems (CHP) based on solid oxide FC (SOFC). An example [59] in which a 1 kWe CHP system was fed by hydrogen stored in a MgH_2 tank thermally coupled with the SOFC stack was discussed in Sections 3.1 and 3.3 above.

4.4. Other applications of metal hydrides in fuel cell systems

Although H_2 storage and supply using the reversible heat-driven interaction of metals or alloys with gaseous H_2 (Reaction 1) is a major representative of MH use in FC applications, there exists a number of interesting developments where other functions of MH's are used. We already mentioned Direct Borohydride Fuel Cells (DBFC) utilising $NaBH_4$ as a fuel and, in some cases, intermetallic hydrides as electrode catalysts [6–8]; hydrogen supply systems where H_2 is generated by hydrolysis of complex hydrides [58]; as well as Alkaline Fuel Cells (AFC) where MH's combine the functions of the hydrogen storage medium and anode catalyst [30]. The electrochemical applications similar to the latter one seem to be particularly promising and will be briefly discussed below.

Fang et al. [183] reported on the use of a TiVCr hydrogen storage alloy coating onto the anode Gas Diffusion Layer (GDL) of a PEM FC by direct-current sputtering. The Membrane Electrode Assemblies (MEA) with the TiVCr-coated GDL exhibited 90.6% greater durability under no-hydrogen flow conditions than the MEA without the TiVCr hydrogen storage alloy coating. These results demonstrated that GDL's coated with a MH may be directly used in PEM FC's to improve their performance and durability.

A prototype reversible PEM FC with integrated MH hydrogen storage was demonstrated by Andrews and Mohammadi [184]. The AB_5-type MH powder was either packed (cold pressed) on the hydrogen side of the MEA, or directly introduced in a MH–nafion composite electrode. As a result, a novel concept for a proton flow battery; a reversible PEM FC with an integrated solid-state MH storage electrode that can be used to store and re-supply electrical energy without formation of H_2 gas, has been developed.

A Metal Hydride Fuel Cell (MHFC) technology in which the MH is embedded in the anode of AFC [185] was successfully scaled up and demonstrated in 320 W stacks and 500 W systems by Ovonic Fuel Cell Company [186]. The stacks had power densities and specific powers over 100 W L^{-1} and 100 W kg^{-1}, respectively, and exhibited durability exceeding 7000 operating hours. It was shown that MHFC's offer a practical, low cost approach to power systems for UPS/emergency power applications.

The integration of MH's into the hydrogen electrode of alkaline electrochemical system was further elaborated by Choi et al. [187] who

proposed a reversible water electrolysis/power generation system based on a FC/battery. The energy conversion efficiencies of hydrogen production and of the complete hydrogen production/power generation process at a current density of 37.0 A m^{-2} were 98.3% and 79.6%, respectively. These values are higher than those of conventional water electrolysis and/or power generation systems.

5. Conclusions

Metal and intermetallic hydrides are utilised for efficient, safe and flexible hydrogen storage systems and can be broadly applied to various stationary, mobile and portable power applications, providing gaseous hydrogen fuel to fuel cells reaching up to several hundred kW in electrical power. Thermal integration of "low temperature" metal hydrides based on AB_5- and AB_2-type intermetallics allows utilisation of up to 40–45% of the heat produced during operation of the FC stack, thus improving the overall system efficiency.

The current system developments are focused on the improvement of hydrogen charge/discharge dynamics by the optimisation of heat distribution and design parameters of the MH beds.

The most promising applications for the "low-temperature" MH's include hydrogen storage for portable and weight efficient mobile applications where individual MH cartridges/canisters can be easily refilled or replaced once depleted, and, hydrogen supply systems for emission-free heavy duty applications, such as forklifts, mining vehicles and marine applications. Other applications also include high-temperature solid oxide FC's, utilising "high-temperature" MH's (e.g., catalysed MgH_2) where up to 90% of the released heat is used, thus achieving an efficient thermal control of the stack.

Finally, the use of metal hydrides in hydrogen electrodes provides opportunities for other promising applications of MH's in FC technologies such as regenerative electrolysers – FC's.

Acknowledgements

The South African co-authors acknowledge financial support of Department of Science and Technology (DST) in South Africa within on-going HySA Systems projects KP3-S02, KP3-S03 and KP8-S05. This work was also supported by Impala Platinum Limited / South Africa. Investment from the industrial funder has been leveraged through the Technology and Human Resources for Industry Programme, jointly managed by the South African National Research Foundation and the Department of Trade and Industry (NRF/DTI; THRIP Project TP1207254249).

This work is also supported by ERAfrica EU FP7 program, project RE-037 "HENERGY". Finally, ML acknowledges the support of South African National Research Foundation (NRF) via incentive funding grant 76735.

The authors are grateful to Professor Ying Wu for his valuable help during the preparation of this manuscript.

References

[1] M. Haug. Energy perspectives: future energy requirements and the role for hydrogen, in: Proceedings of the 1st European Hydrogen Energy Conference, Grenoble, 2–5 September 2003.
[2] R.M. Dell, D.A.J. Rand, J. Power Sources 100 (2001) 2–17.
[3] C.H. Chao, J.J. Shieh, Int. J. Hydrogen Energy 37 (2012) 13141–13146.
[4] F. Barbir, PEM Fuel Cells: Theory and Practice, second ed, Elsevier/Academic Press, 2013.
[5] S.P.S. Badwal, S.S. Giddey, C. Munnings, A.I. Bhatt, A.F. Hollenkamp, Emerging electrochemical energy conversion and storage technologies, Front. Chem. 2 (2014) 79. http://dx.doi.org/10.3389/fchem.2014.00079.
[6] J. Ma, N.A. Choudhury, Y. Sahai, Renew. Sustain. Energy Reviews 14 (2010) 183–199.
[7] J. Ma, N.A. Choudhury, Y. Sahai, R.G. Buchheit, Fuel Cells 11 (5) (2011) 603–610. http://dx.doi.org/10.1002/fuce.201000125.
[8] J.H. Wee, J. Power Sources 161 (2006) 1–10.
[9] D.P. Kothari, K.C. Singal, R. Ranjan, Renewable Energy Sources and Emerging Technologies, second ed, PHI Learning Private Limited, 2011.
[10] A. Chandan, M. Hattenberger, A. El-kharouf, S. Du, A. Dhir, V. Self, B.G. Pollet, A. Ingrama, W. Bujalski, J. Power Sources 231 (2013) 264–278.
[11] Nedstack PEM Fuel Cells; downloaded from ⟨http://www.nedstack.com/technology/fuel-cell-types⟩.
[12] Fuel Cell Handbook, NovemberEG & G Technical Services, Seventh Edition, Inc. U.S. Department of Energy, 2004.
[13] S. Hardman, A. Chandan, R. Steinberger-Wilckens, J. Power Sources 287 (2015) 297–306.
[14] B.P. Tarasov, M.V. Lototskii, Russ. J. Gen. Chem. 77 (4) (2007) 660–675.
[15] J. Andrews, B. Shabani, Int. J. Hydrogen Energy 37 (2012) 1184–1203.
[16] L. Schlapbach, A. Züttel, Nature 414 (2001) 353–358.
[17] E. Tzimas, C. Filiou, S.D. Peteves, J.-B. Veyret, EUR 20995 EN - Hydrogen Storage: State-of-the-art and future perspective, European Communities (2003) downloaded from ⟨http://www.jrc.nl/publ/P2003-181=EUR20995EN.pdf⟩.
[18] A. Züttel, P. Wenger, P. Sudan, P. Mauron, S.I. Orimo, Mater. Sci. Eng. B108 (2004) 9–18.
[19] A. Züttel, Materials Today 6 (9) (2003) 24–33.
[20] V.A. Yartys, M.V. Lototsky, An overview of hydrogen storage methods, in: T.N. Veziroglu, S.Y. Zaginaichenko, D.V. Schur, B. Baranowski, A.P. Shpak, V.V. Skorokhod (Eds.), Hydrogen Materials Science and Chemistry of Carbon Nanomaterials, Kluwer Acad. Publ., 2004, pp. 75–104.
[21] B.P. Tarasov, M.V. Lototskii, V.A. Yartys', Russ. J. Gen. Chem. 77 (4) (2007) 694–711.
[22] A. Godula-Jopek, Hydrogen Storage Options Including Constraints and Challenges, in: A. Godula-Jopek (Ed.)Hydrogen Production: by ElectrolysisFirst Edition, Wiley-VCH Verlag GmbH & Co. KGaA, 2015, pp. 273–309.
[23] P. Millet, Hydrogen storage in hydride-forming materials, in: A. Basile, A. Iulianelli (Eds.), Advances in Hydrogen Production, Storage and Distribution, Elsevier, 2014, pp. 368–409. http://dx.doi.org/10.1533/9780857097736.3.368.
[24] M. Lototskyy, V.A. Yartys, J. Alloys Compds. 645 (2015) S365–S373.
[25] P. Dantzer, Metal-hydride technology: a critical review, in: H. Wipf (Ed.)Hydrogen in metals III. Properties and applications. Berlin-Heidelberg, Springer-Verlag, 1997, pp. 279–340.
[26] G. Sandrock, J. Alloys Compds 293–295 (1999) 877–888.
[27] G. Sandrock, R.C. Bowman Jr., J. Alloys Compds 356-357 (2003) 794–799.
[28] M.V. Lototskyy, V.A. Yartys, B.G. Pollet, R.C. Bowman Jr., Int. J. Hydrogen Energy 39 (2014) 5818–5851.
[29] M. Lototskyy, B. Satya Sekhar, P. Muthukumar, V. Linkov, B.G. Pollet, J. Alloys Compds 645 (2015) S117–S122.
[30] C. Wang, A.J. Appleby, D.L. Cocke, J. Electrochem. Soc. 151 (2) (2004) A260–A264.
[31] E.MacA. Gray, C.J. Webb, J. Andrews, B. Shabani, P.J. Tsai, S.L.I. Chan, Int. J. Hydrogen Energy 36 (2011) 654–663.
[32] A.R. Miedema, K.H.J. Buschow, H.H. Van Mal, J Less-Common Met. 49 (1976) 463–472.
[33] S. Luo, W. Luo, J.D. Clewley, T.B. Flanagan, R.C. Bowman Jr., J. Alloys Compds 231 (1995) 473–478.
[34] M.V. Lototskyy, Int. J. Hydrogen Energy 41 (2016) 2739–2761.
[35] D. Chabane, F. Harel, A. Djerdir, D. Candusso, O. ElKedim, N. Fenineche, Int. J. Hydrogen Energy 41 (2016) 11682–11691.
[36] S.P. Malyshenko, S.V. Mitrokhin, I.A. Romanov, J. Alloys Compds 645 (2015) S84–S88.
[37] S.S. Mohammadshahi, T.A. Webb, E. MacA.Gray, C.J. Webb. Experimental and theoretical study of compositional inhomogeneities in $LaNi_5D_x$ owing to temperature gradients and pressure hysteresis, in: Proceedings of the 15th Int. Symp. On Metal – Hydrogen Systems, MH2016, 7-12Aug. 2016, Interlaken, Switzerland, presentation AB000645.
[38] C. Song, L.E. Klebanoff, T.A. Johnson, B.S. Chao, A.F. Socha, J.M. Oros, C.J. Radley, S. Wingert, J.S. Breit, Int. J. Hydrogen Energy 39 (2014) 14896–14911.
[39] B. Bogdanović, R.A. Brand, A. Marjanović, M. Schwickardi, J. Tölle, J. Alloys Compds 302 (2000) 36–58.
[40] J.M. Pasini, C. Corgnale, B.A. van Hassel, T. Motyka, S. Kumar, K.L. Simmons, Int. J. Hydrogen Energy 38 (2013) 9755–9765.
[41] H. Nakano, S. Wakao, T. Shimizu, J. Alloys Compds 254 (1997) 609–612.
[42] P. Dantzer, Mater. Sci. Eng. A 329-331 (2002) 313–320.
[43] M.V. Lototskyy, M.W. Davids, I. Tolj, Y.V. Klochko, B. Satya Sekhar, S. Chidziva, F. Smith, D. Swanepoel, B.G. Pollet, Int. J. Hydrogen Energy 40 (2015) 11491–11497.
[44] M.V. Lototskyy, I. Tolj, M.W. Davids, Y.V. Klochko, A. Parsons, D. Swanepoel, R. Ehlers, G. Louw, B. van der Westhuizen, F. Smith, B.G. Pollet, C. Sita, V. Linkov, Int. J. Hydrogen Energy 41 (2016) 13831–13842.
[45] C. Zhou, Z.Z. Fang, R.C. Bowman Jr., J. Phys. Chem. C 119 (39) (2015) 22261–22271.
[46] M. Lototskyy, J.M. Sibanyoni, R.V. Denys, M. Williams, B.G. Pollet, V.A. Yartys, Carbon 57 (2013) 146–160.
[47] M. Lototskyy, M.W. Davids, J.M. Sibanyoni, J. Goh, B.G. Pollet, J. Alloys Compds 645 (2015) S454–S459.
[48] R.K. Ahluwalia, J.K. Peng, T.Q. Hua, Int. J. Hydrogen Energy 39 (2014) 14874–14886.
[49] United States Department of Energy. Targets for onboard hydrogen storage systems for light-duty vehicles (2012) Downloaded from: ⟨http://energy.gov/eere/fuelcells/downloads/doe-targets-onboard-hydrogen-storage-systems-light-duty-vehicles⟩.
[50] D. Wenger, W. Polifke, E. Schmidt-Ihn, T. Abdel-Baset, S. Maus, Int. J. Hydrogen

Energy 34 (2009) 6265–6270.
[51] J.-L. Bobet, B. Darriet, Int. J. Hydrogen Energy 25 (2000) 767–772.
[52] L. Pickering, J. Li, D. Reed, A.I. Bevan, D. Book, J. Alloys Compds 508 (2013) S233–S237.
[53] B.D. MacDonald, A.M. Rowe, J. Power Sources 161 (2006) 346–355.
[54] A.R. Miller, D.L. Barnes. Advanced underground vehicle power and control fuel cell mine locomotive, in: Proc. of the 2002 U.S. DOE Hydrogen Program Review NREL/CP-610-32405.
[55] V. Rajpurohit, G. Venkatarathnam, S. Srinivasa Murthy. An analysis of coupled. PEM fuel cell – metal hydride hydrogen storage tank system, in: Proceedings of the 2nd European Conference on Polygeneration – 30th March-1st April, 2011– Tarragona, Spain
[56] K.N. Grew, Z.B. Brownlee, K.C. Shukla, D. Chu, J. Power Sources 217 (2012) 417–430.
[57] J.J. Hwang, W.R. Chang, J.Power Sources 207 (2012) 111–119.
[58] J. Kim, T. Kim, Appl. Energy 160 (2015) 945–953.
[59] B. Delhomme, A. Lanzini, G.A. Ortigoza-Villalba, S. Nachev, P. de Rango, M. Santarelli, P. Marty, P. Leone, Int. J. Hydrogen Energy 38 (2013) 4740–4747.
[60] S. Garrier, A. Chaise, P. de Rango, P. Marty, B. Delhomme, D. Fruchart, S. Miraglia, Int. J. Hydrogen Energy 36 (2011) 9719–9726.
[61] D. Parra, M. Gillott, G.S. Walker, Int. J. Hydrogen Energy 41 (2016) 5215–5229.
[62] J.M. Moore, J.B. Lakeman, G.O. Mepsted, J. Power Sources 106 (2002) 16–20.
[63] T.M. Keränen, H. Karimäkia, J. Viitakangas, J. Vallet, J. Ihonen, P. Hyötylä, H. Uusalo, T. Tingelöf, J. Power Sources 196 (2011) 9058–9068.
[64] F. Weng, J.-Y. Chen, A. Su, S.-H. Chan. Development of metal plate fuel cell stack system as a range extender of tourist LEV, in: 26th Electric Vehicle Symposium 2012, EVS 2012, 2, pp. 1472-1476
[65] S.K. Khaitan, M. Raju, Int. J. Hydrogen Energy 37 (2012) 2344–2352.
[66] M. Raju, S. Khaitan, Int. J. Hydrogen Energy 36 (2011) 10797–10807.
[67] M. Lototskyy, I. Tolj, M.W. Davids, P. Bujlo, F. Smith, B.G. Pollet, J. Alloys Compds 645 (2015) S329–S333.
[68] E.I. Gkanas, S.S. Makridis, Int. J. Hydrogen Energy 41 (2016) 5693–5708.
[69] N.-C. Shih, C.-L. Lin, C.-C. Chang, D.-Y. Wang, Int. J. Hydrogen Energy 38 (2013) 11144–11148.
[70] M. Baricco. SSH2S (256653): Fuel Cell Coupled Solid State Hydrogen Storage Tank, downloaded at ⟨http://www.fch.europa.eu/sites/default/files/2.%20M.BARICCO-SSH2S%20(ID%20193364)%20(ID%20193813).pdf⟩
[71] S. Krummrich. Fuel Cell Methanol Reformer System for Submarines, in: D. Stolten, T. Grube (Eds.): 18th World Hydrogen Energy Conference 2010, Parallel Sessions Book 3: Hydrogen Production Technologies - Part 2 in: Proceedings of the WHEC2010, May 16-21, 2010, Essen, pp. 213-218.
[72] L.E. Klebanoff, J.S. Breit, G.S. Roe, T. Damberger, T. Erbel, S. Wingert, et al., Int. J. Hydrogen Energy 39 (2014) 12948–12972.
[73] M. Kickulies, Fuel Cells Bull. (2005) 12–15.
[74] Fuel cell scooters, solar hydrogen station launched in Hawaii, Fuel Cells Bull. (2012) 7
[75] P. Valicek, F. Fourie. Fuel cell technology in underground mining, in: The 6th International Platinum Conference, 'Platinum–Metal for the Future', The SouthernAfrican Institute of Mining and Metallurgy, 2014, pp. 325_332.
[76] V. Güther, A. Otto, J. Alloys Compds 293-295 (1999) 889–892.
[77] R. Urbanczyk,D. Bathen, M. Felderhoff, J. Burfeind. HT-PEM fuel cell system with integrated complex hydride storage tank, in: D. Stolten, T. Grube (Eds.): 18th World Hydrogen Energy Conference 2010, Parallel Sessions Book 4: Storage Systems / Policy Perspectives, Initiatives and Co-operations: Proceedings of the WHEC2010, May 16-21, 2010, Essen, pp. 177-183
[78] S. Nižetić, I. Tolj, A.M. Papadopoulos, Energy Conversion and Management 105 (2015) 1037–1045.
[79] G.L. Guizzi, M. Manno, M. De Falco, Int. J. Hydrogen Energy 34 (2009) 3112–3124.
[80] E. Varkaraki, N. Lymberopoulos, A. Zachariou, J. Power Sources 118 (2003) 14–22.
[81] G. Andreasen, M. Melnichuk, S. Ramos, H.L. Corso, A. Visintin, W.E. Triaca, H.A. Peretti, Int. J. Hydrogen Energy 38 (2013) 13352–13359.
[82] G. Doucet, C. Etiévant, C. Puyenchet, S. Grigoriev, P. Millet, Int. J. Hydrogen Energy 34 (2009) 4983–4989.
[83] P. Rizzi, E. Pinatel, C. Luetto, P. Florian, A. Graizzaro, S. Gagliano, M. Baricco, J. Alloys Compds 645 (2015) S338–S342.
[84] P.R. Wilson, R.C. Bowman Jr., J.L. Mora, J.W. Reiter, J. Alloys Compds 446-447 (2007) 676–680.
[85] C. Corgnale, T. Motyka, S. Greenway, J.M. Perez-Berrios, A. Nakano, H. Ito, T. Maeda, J. Alloys Compds 580 (2013) S406–S409.
[86] B. Shabani, J. Andrews, A. Subic, B. Paul. Novel concept of long-haul trucks powered by hydrogen fuel cells, in: SAE-China and FISITA (eds.), Proc. FISITA 2012 World Automotive Congress, Lecture Notes in Electrical Engineering 192, Springer-Verlag Berlin Heidelberg, 2013, pp.823-834.
[87] J. Farnes, A. Vik, D. Bokach, T. Svendsen, M. Schautz, X. Geneste. Recent developments of regenerative fuel cell systems for satellites, in: Proc. '10th European Space Power Conference', Noordwijkerhout, The Netherlands, 15–17 April 2014 (ESA SP-719, May 2014), downloaded at ⟨http://www.esa-tec.eu/workspace/assets/files/tdo0157-paper-regenerative-f-5504a3929eb6a.pdf⟩.
[88] A. Reissner, R.H. Pawelke, S. Hummel, D. Cabelka, J. Gerger, J. Farnes, A. Vik, I. Wernhus, T. Svendsen, M. Schautz, X. Geneste, J. Alloys Compds 645 (2015) S9–S13.
[89] B.P. Tarasov, Int. J. Hydrogen Energy 36 (2011) 1196–1199.
[90] T. Maeda, K. Nishida, M. Tange, T. Takahashi, A. Nakano, H. Ito, Y. Hasegawa, M. Masuda, Y. Kawakami, Int. J. Hydrogen Energy 36 (2011) 10845–10854.
[91] A. Nakano, T. Maeda, H. Ito, T. Motyka, J.M. Perez-Berrios, S. Greenway, Energy Procedia 29 (2012) 463–468.
[92] F. Fang, Y. Li, Q. Zhang, L. Sun, Z. Shao, D. Sun, J. Power Sources 195 (2010) 8215–8221.
[93] Y. Chen, C.A.C. Sequeira, C. Chena, X. Wang, Q. Wang, Int. J. Hydrogen Energy 28 (2003) 329–333.
[94] S. Lévesque, M. Ciureanu, R. Roberge, T. Motyka, Int. J. Hydrogen Energy 25 (2000) 1095–1105.
[95] D.R. Hsiao, B.W. Huang, N.C. Shih, Int. J. Hydrogen Energy 37 (2012) 1058–1066.
[96] R. Maceiras, V. Alfonsin, A. Cancela, A. Sanchez, Eur J Sustain Development 4 (2015) 129–134.
[97] M.V. Lototskyy, I. Tolj, A. Parsons, F. Smith, C. Sita, V. Linkov, J. Power Sources 316 (2016) 239–250.
[98] M. Fuchs, F. Barbir, M. Nadal. Performance of Third Generation Fuel Cell Powered Utility Vehicle #2 with Metal Hydride Fuel Storage, in: Proceedings of the 2001 European PE Fuel Cell Forum, Luzern, Switzerland, July 2-6 2001
[99] L.K. Heung, T. Motyka, W.A. Summers. Hydrogen Storage Development for Utility Vehicles, in: Proceedings of the 4th International Symposium on Hydrogen Power – Theoretical and Engineering Solutions, 9-14 September 2001, pp.336-341.
[100] P. Pfeifer, C. Wall, O. Jensen, H. Hahn, M. Fichtner, Int. J. Hydrogen Energy 34 (2009) 3457–3466.
[101] M. Nasri, D. Dickenson. Thermal Management of Fuel Cell-driven Vehicles using HT-PEM and Hydrogen Storage, in: Proceedings of Ninth International Conference on Ecological Vehicles and Renewable Energies, Monte-Carlo, 25-27th March 2014, pp.1-6.
[102] E.H. Reddy, S. Jayanti, Energy Procedia 29 (2012) 254–264.
[103] A.P. Tetuko, B. Shabani, J. Andrews, Int. J. Hydrogen Energy 41 (2016) 4264–4277.
[104] T. Førde, J. Eriksen, A.G. Pettersen, P.J.S. Vie, Ø. Ulleberg, Int. J. Hydrogen Energy 34 (2009) 6730–6739.
[105] J.P. Vanhanen, P.D. Lund, M.T. Hangström, Int. J. Hydrogen Energy 21 (1996) 213–221.
[106] S. Pedrazzi, G. Zini, P. Tartarini, Renew. Energy 46 (2012) 14–22.
[107] D. Mori, K. Hirose, N. Haraikawa, T. Takiguchi, T. Shinozawa, T. Matsunaga, K. Toh, K. Fujita, A. Kumano, H. Kubo. High-pressure Metal Hydride Tank for Fuel Cell Vehicles, in: Proceedings of the JSAE/SAE International Fuels & Lubricants Meeting, 2007, SAE 2007-01-2011, pp.560-564.
[108] A.G. Yiotis, M.E. Kainourgiakis, L.I. Kosmidis, G.C. Charalambopoulou, A.K. Stubos, J. Power Sources 269 (2014) 440–450.
[109] R. Pedicini, A. Saccà, A. Carbone, E. Passalacqua, Int. J. Hydrogen Energy 36 (2011) 9062–9068.
[110] R. Pedicini, F. Matera, G. Giacoppo, I. Gatto, E. Passalacqua, Int. J. Hydrogen Energy 40 (2015) 17388–17393.
[111] K. Yvon. New metal hydrides for hydrogen storage in PEM fuel cell systems, Project report (Im Auftrag des Bundesamt für Energie, Forschungsprogramm Brennstoffzellen inkl. Wasserstoff; Projektnummer: 101812), Eidgenössisches Departement für Umwelt, Verkehr, Energie und Kommunikation UVEK, 2007; downloaded from ⟨http://www.bfe.admin.ch⟩.
[112] N.A.A. Rusman, M. Dahari, Int. J. Hydrogen Energy 41 (2016) 12108–12126.
[113] D.-W. Sun, Int. J. Hydrogen Energy 17 (12) (1992) 945–949.
[114] F.S. Yang, G.X. Wang, Z.X. Zhang, X.Y. Meng, V. Rudolph, Int. J. Hydrogen Energy 35 (2010) 3832–3840.
[115] S. Shafiee, M.H. McCay, Int. J. Hydrogen Energy 41 (2016) 9462–9470.
[116] A. Mazzucco, M. Dornheim, M. Sloth, T.R. Jensen, J.O. Jensen, M. Rokni, Int. J. Hydrogen Energy 39 (2014) 17054–17074.
[117] JMCUSA H2 Storage Systems, ⟨http://www.jmcusa.com/mh3.htm⟩
[118] E.I. Gkanas, S.S Makridis, E.S. Kikkinides, A.K. Stubos. Perforation Effect on a Rectangular Metal Hydride Tank for the Hydriding and Dehydriding Process by Using COMSOL Multiphysics Software, Excerpt from the Proceedings of the 2012 COMSOL Conference in Milan, ⟨https://arxiv.org/ftp/arxiv/papers/1303/1303.4512.pdf⟩.
[119] C.A. Krokos, D. Nikolic, E.S. Kikkinides, M.C. Georgiadis, A.K. Stubos, Int. J. Hydrogen Energy 34 (2009) 9128–9140.
[120] T. Sakai, N. Honda, I. Yonezu. Metal hydride container and metal hydride heat storage system, Patent US 4510759 (1985).
[121] S.R. Ovshinsky, R.T. Young, Y. Li, V. Myasnikov, V. Sobolev. Hydrogen storage bed system including an integrated thermal management system, Patent US 6833118 B2 (2004).
[122] S. Garrier, B. Delhomme, P. de Rango, P. Marty, D. Fruchart, S. Miraglia, Int. J. Hydrogen Energy 38 (2013) 9766–9771.
[123] S. Mellouli, H. Dhaou, F. Askri, A. Jemni, S. Ben Nasrallah, Int. J. Hydrogen Energy 34 (2009) 9393–9401.
[124] F. Laurencelle, J. Goyette, Int. J. Hydrogen Energy 32 (2007) 2957–2964.
[125] F. Askri, M. Ben Salah, A. Jemni, S. Ben Nasrallah, Int. J. Hydrogen Energy 34 (2009) 897–905.
[126] M. Nagel, Y. Komazaki, S. Suda, J. Less-Common Met. 120 (1986) 35–43.
[127] M. Ron, D. Gruen, M. Mendelsohn, I. Sheet, J. Less-Common Met. 74 (2) (1980) 445–448.
[128] E. Bershadsky, Y. Josephy, M. Ron, J. Less-Common Met. 153 (1989) 65–78.
[129] K.J. Kim, B. Montoya, A. Razani, K.-H. Lee, Int. J. Hydrogen Energy 26 (2001) 609–613.
[130] A.R. Sanchez, H.-P. Klein, M. Groll, Int. J. Hydrogen Energy 28 (2003) 515–527.
[131] K.J. Kim, K.T. Feldman Jr, G. Lloyd, A. Razani, K.L. Shanahan, Int. J. Hydrogen Energy 23 (5) (1998) 355–362.

[132] B. Satya Sekhar, M. Lototskyy, A. Kolesnikov, M.L. Moropeng, B.P. Tarasov, B.G. Pollet, J. Alloys Compds 645 (2015) S89–S95.
[133] M. Lototskyy, V. Linkov. Hydride container, Patent ZA 2009/02427.
[134] H.-P. Klein, M. Groll, Appl. Therm. Eng. 22 (2002) 631–639.
[135] B. Delhomme, P. de Rango, P. Marty, M. Bacia, B. Zawilski, C. Raufast, S. Miraglia, D. Fruchart, Int. J. Hydrogen Energy 37 (2012) 9103–9111.
[136] P. Muthukumar, A. Singhal, G.K. Bansal, Int. J. Hydrogen Energy 37 (2012) 14351–14364.
[137] M. Visaria, I. Mudawar, Int. J. Hydrogen Energy 37 (2012) 5735–5749.
[138] S. Mellouli, F. Askri, H. Dhaou, A. Jemni, S. Ben Nasrallah, Int. J. Hydrogen Energy 35 (2010) 1693–1705.
[139] A.O. Lukman, O.B. Abiodun, O. Sadiku-Agboola, P.A. Popoola, E.R. Sadiku, J. Chem. Chem. Eng. 6 (2012) 604–612.
[140] F. Grote, P. Busse, V. Guther, A. Otto. Tank for the reversible storage of hydrogen, Patent application US 2003/0167923 Al.
[141] H. Suzuki, H. Ishikawa, K. Oguro, A. Kato, T. Okada; S. Sakamoto, H. Kawashima, K. Sakaguchi. Reactor with hydrogen adsorption alloy, Patent US 5019358 (1991).
[142] P.De Rango, A.Chaise, D.Fruchart, P.Marty, S.Miraglia. Hydrogen storage tank, Patent application US 2010/0326992 A1.
[143] T. Fuura, S. Tsunokake, M. Monde, Y. Sakaguchi, N. Sakaguchi, H. Nishiwaki, Y. Maeda, K. Moriya, S. Watanabe, JARI Res. J. 28 (7) (2006) 63–68.
[144] S. Lasher. Analyses of Hydrogen Storage Materials and On-Board Systems, DOE Merit Review, May 25, 2005, Project ID #ST19, ⟨www.hydrogen.energy.gov/pdfs/review05/st19_lasher.pdf⟩.
[145] D. Mori, Y. Kimura, T. Nito, M. Kimbara, T. Shinozawa, K. Toh, H. Kubo. Hydrogen-storage container and method of occluding hydrogen, Patent application EP1 384 940 A2 (2005).
[146] D. Mori, N. Haraikawa, N. Kobayashi, T. Shinozawa, T. Matsunaga, H. Kubo, K. Toh, M. Tsuzuki. High-pressure metal hydride tank for fuel cell vehicles, in: Proceedings of the IPHE Int. Hydrogen Storage Conf., 19-22 June 2005, Lucca, Italy, ⟨http://www.iphe.net/docs/Meetings/Lucca_Italy_05/Daigoro_Mori.pdf⟩.
[147] M.V. Lototskyy, D. Swanepoel, M.W. Davids, Y. Klochko, B.J. Bladergroen, V.M. Linkov. Multistage metal hydride hydrogen compressor, Patent application PCT/IB2016/051493 (ZA2015/01837).
[148] J.-H. Cho, S.-S. Yu, M.-Y. Kim, S.-G. Kang, Y.-D. Lee, K.-Y. Ahn, H.-J. Ji, Int. J. Hydrogen Energy 38 (2013) 8813–8828.
[149] T. Brestovič, N. Jasminská, R. Pyszko, M. Lázár, M. Puškár, Measurement 72 (2015) 52–60.
[150] S.S. Mohammadshahi, E.MacA. Gray, C.J. Webb, Int. J. Hydrogen Energy 41 (2016) 3470–3484.
[151] K.C. Smith, T.S. Fisher, Int. J. Hydrogen Energy 37 (2012) 13417–13428.
[152] K. Nasako, Y. Ito, N. Hiro, M. Osumi, J. Alloys Compds 264 (1998) 271–276.
[153] M. Okumura, K. Terui, A. Ikado, Y. Saito, M. Shoji, Y. Matsushita, H. Aoki, T. Miura, Y. Kawakami, Int. J. Hydrogen Energy 37 (2012) 6686–6693.
[154] R. Schulz, G. Liang, J. Huot, P. Larochelle. Method for storing hydrogen in hybrid form, Patent application WO 2005/064227 Al.
[155] H. Tsuruta, T. Yokota, T. Okita, T. Takano, N. Kuriyama, N. Takeichi. Hybrid type hydrogen storage vessel, Patent JP2006307959 A.
[156] T. Yokota, K. Hamada, H. Tsuruta, N. Kuriyama, H. Takeshita, N. Takeichi, T. Takano. Hybrid hydrogen storage container and method of storing hydrogen in container, Patent US 7681753 B2 (2010).
[157] Z. Jiang, R.A. Dougal, S. Liu, S.A. Gadre, A.D. Ebner, J.A. Ritter, J. Power Sources 142 (2005) 92–102.
[158] M.W. Davids, I. Tolj, T.-C. Jao, M. Lototskyy, S. Pasupathi, C. Sita, ECS Trans. 75 (14) (2016) 553–562.
[159] V. Myasnikov, R. Young, Y. Li, S.R. Ovshinsky. Onboard hydrogen storage unit with heat transfer system for use in a hydrogen powered vehicle, Patent US 6918430 B2 (2005).
[160] M. Lototskyy, I. Tolj, M.W. Davids, B.G. Pollet, V. Linkov. Hydrogen storage and supply system integrated with fuel cell power pack, Patent ZA2014/08640.
[161] J. Fernández-Moreno, G. Guelbenzu, A.J. Martín, M.A. Folgado, P. Ferreira-Aparicio, A.M. Chaparro, Appl. Energy 109 (2013) 60–66.
[162] H.S. Han, C. Cho, S.Y. Kim, J.M. Hyun, Appl. Energy 105 (2013) 125–137.
[163] S.H. Kim, C.M. Miesse, H.B. Lee, I.W. Chang, Y.S. Hwang, J.H. Jang, S.W. Cha, Appl. Energy 134 (2014) 382–391.
[164] F. Gonzatti, V. Nizolli, F.Z. Ferrigolo, F.A. Farret, M.A. Silva de Mello, Int. J. Emerg. Electr. Power Syst. 17 (1) (2016) 59–67.
[165] Ovonic Hydrogen Solutions, leaflet, downloaded at ⟨http://www.ovonic-hydrogen.com⟩.
[166] B.S. Chao, R.C. Young, V. Myasnikov, Y. Li, B. Huang, F. Gingl, P.D. Ferro, V. Sobolev, S.R. Ovshinsky. Recent Advances in Solid Hydrogen Storage Systems, downloaded at ⟨http://www.ovonic.com/res/2_4_solid_hydrogen/publications.htm⟩.
[167] J.P. Vanhanen, P.D. Lund, J.S. Tolonen, Int. J. Hydrogen Energy 23 (1998) 267–271.
[168] A. Jossen, J. Garche, H. Doering, M. Goetz, W. Knaupp, L. Joerissen, J. Power Sources 144 (2005) 395–401.
[169] E.I. Gkanas, S.S. Makridis, A.K. Stubos. Coupling thermal integration of a solid oxide fuel cell with a magnesium metal hydride tank, downloaded at ⟨https://arxiv.org/ftp/arxiv/papers/1412/1412.0878.pdf⟩.
[170] T.S. Doyle, Z. Dehouche, S. Stankovic, Int. J. Hydrogen Energy 40 (2015) 9013–9025.
[171] V. Hovland. Integrated cabin and fuel cell system thermal management with a metal hydride heat pump, Conference paper, MH2002, Annecy, France, September 2–6, 2002; downloaded at ⟨http://www.osti.gov/bridge⟩.
[172] V. Alfonsín, A. Suarez, A. Cancela, A. Sanchez, R. Maceiras, Int. J. Hydrogen Energy 39 (2014) 11763–11773.
[173] G. Kyriakarakos, A.I. Dounis, S. Rozakis, K.G. Arvanitis, G. Papadakis, Appl. Energy 88 (2011) 4517–4526.
[174] C. Corgnale, T. Motyka, S. Greenway, J. Perez-Berrios, A. Nakano, H. Ito, T. Maeda. Regenerative fuel cell systems with metal hydride storage, for renewable power production, presentation: in: Proceedings of the Fuel Cell Seminar 2012, Uncasville,CT, November 2012, downloaded at ⟨http://fuelcellseminar.com/wp-content/uploads/sta32-2-11.pdf⟩.
[175] V. Iosub, A. Chaise, A. Dufouil, B. Fremon, P. Capron, O. Gillia. Functionalizing the metal hydrides for hydrogen cartridges, in: Proceedings of the 15th Int. Symp. On Metal – Hydrogen Systems, MH2016, 7-12Aug. 2016, Interlaken, Switzerland, presentation AB000940.
[176] I. Tolj, M.V. Lototskyy, M.W. Davids, S. Pasupathi, G. Swart, B.G. Pollet, Int. J. Hydrogen Energy 38 (2013) 10630–10639.
[177] F. Barbir, B. Simic, G. Stipanovic, D. Bezmalinovic. Demonstration of a fuel cell powered boat, in: 18th World Hydrogen Energy Conference 2010 - WHEC 2010Parallel Sessions. Book 6: Stationary Applications / Transportation Applications, pp.269-271.
[178] A.I. Bevan, A. Züttel, D. Book, I.R. Harris, Faraday Discussion 151 (2011) 353–367.
[179] I.K. Landgraf, M. Kasatkin. On the universal approach to development and deployment of fuel cell power plants of various purposes. In: Proceedings of the 13th Int. Meeting “Fundamental Problems of Solid State Ionics”, Russian Federation, Moscow Region, Chernogolovka, June 27 – July 01 2016. Proc. of Meeting, pp. 122-125.
[180] C. Fiori, A. Dell'Era, F. Zuccari, A. Santiangeli, A. D'Orazio, F. Orecchini, Int. J. Hydrogen Energy 40 (2015) 11879–11889.
[181] Toshiba H2One™ Hydrogen Based Autonomous Energy Supply System Now Providing Power to a Kyushu Resort Hotel, Toshiba Press Release (14 Mar, 2016), ⟨http://www.toshiba.co.jp/about/press/2016_03/pr1402.htm⟩.
[182] T. Kono. New Hydrogen Energy Supply System by using a Hydrogen Storage Alloy, 15th Int. Symp. On Metal – Hydrogen Systems, MH2016, 7-12Aug. 2016, Interlaken, Switzerland, presentation AB001590.
[183] S.-Y. Fang, R.-H. Huang, L.G. Teoh, K.-L. Hsueh, W.-K. Chao, D.-C. Tsai, T.-N. Yang, F.-S. Shieu, J. Power Sources 268 (2014) 443–450.
[184] J. Andrews, S.S. Mohammadi, Int. J. Hydrogen Energy 39 (2014) 1740–1751.
[185] S.R. Ovshinsky, S. Venkatesan, B. Aladjov, R.T. Young, T. Hopper. Alkaline fuel cell, Patent US 6447942 Bl (2002).
[186] K. Fok. Recent advances in metal hydride fuel cell technology for UPS/emergency power applications, downloaded at ⟨www.battcon.com/papersfinal2007/fokpaper2007.pdf⟩.
[187] B. Choi, D. Panthi, M. Nakoji, T. Kabutomori, K. Tsutsumi, A. Tsutsumi, Int. J. Hydrogen Energy 40 (2015) 6197–6206.